



UiT The Arctic University of Norway

Faculty of Bioscience, Fisheries, and Economics, Department for Arctic and Marine Biology

## **Let it glow! Adapting a method to detect microplastics in snow and evaluate the potential for long-range transport**

Vegard Stürzinger

Master's thesis in Biology, BIO3950, May 2020





Master student: **Vegard Stürzinger**<sup>1,2,3</sup>

Main supervisor: **Sophie Bourgeon**<sup>1</sup>

Co-supervisor: **Ingeborg Hallanger**<sup>2</sup>

Co-supervisor: **Dorte Hertzke**<sup>3</sup>

Internal sensor: **Anita Evenset**<sup>4</sup>

External sensor: **Mats Bjørkman**<sup>5</sup>

<sup>1</sup> University in Tromsø, <sup>2</sup> Norwegian Polar Institute, <sup>3</sup> Norwegian Institute for Air Research, <sup>4</sup> Akvaplan NIVA, <sup>5</sup> University of Gothenburg





## **Acknowledgments**

First and foremost, I would like to express my gratitude to my supervisors, Sophie Bourgeon, Ingeborg Hallanger, and Dorte Hertzke. They guided me through my master thesis, even in trying times, and provided me with an opportunity to go to China to meet my Chinese counterparts. I would like to thank J-C Gallet for his advice on snow sampling and providing me with tips and equipment. Special mentions to Ivan for helping me with sampling the snow and Mathea for supporting me even though I was going through darker times in my life.

Thank you for the ride to my friends who have been writing their thesis alongside me. I am grateful to the Norwegian Polar Institute for providing an office with great people for lunches, sporadic help, and Friday beers. A big thank you to the Norwegian Institute for Air Research, Tromsø for providing me with laboratory facilities and knowledge that helped me along the way. Finally, a mention to Geir W. Gabrielsen for introducing me to Ingeborg for this master thesis.



## Abstract

Harmonization of methods in microplastics research is lacking; this is affecting the comparability of results and hindering reproducibility. Investigating microplastics in snow is a relatively new field of research, and it can be used to answer questions about long-range atmospheric transport of microplastics. In this thesis, snow sampling methods were combined with the dye, Nile Red, to develop a method to identify and quantify microplastics in snow. There was an emphasis on quality control and quality assurance, and blank samples were taken throughout the sampling and laboratory procedures. To test and validate the method, a study was performed in northern Norway to compare urban and rural locations. In addition to the field samples, laboratory testing was done by staining known plastic polymers and excluding possible staining of different organic material occurring in snow. We found that the urban locations contained a significantly higher mean number of microplastics per liter of snow compared to rural locations,  $694 \pm 375$  (mean  $\pm$  S.E.) particles L<sup>-1</sup> snow vs.  $432 \pm 386$  particles L<sup>-1</sup> snow, respectively. The most substantial proportion of microplastics was in the lowest size class (22-50  $\mu$ m) for both rural and urban locations. This protocol provides a simple and effective method that can be applied anywhere and could increase the comparability of results.

**Keywords:** Nile Red, Quality Assurance, Protocol development, Arctic, Stereomicroscope.





## **List of abbreviations**

LED - Light Emitting Diodes

NR - Nile Red

MP - Microplastic

WP550 - Whirl-Pak 550

LRT – Long-range transport

MDL – Method detection limit

FTIR - Fourier transform infrared spectroscopy

SD – Standard deviation

DD – Decimal degrees

QA – Quality Assurance

QC – Quality Control



# Table of contents

Acknowledgments .....	iii
Abstract .....	v
List of abbreviations .....	vii
Table of contents .....	ix
1 Introduction .....	1
1.1 Plastic pollution- sources and size classes of particles.....	1
1.2 Pathways .....	3
1.3 Methodological limitations in MP research.....	5
1.4 Thesis description.....	5
2 Materials and methods .....	7
2.1 Sampling strategy.....	7
2.2 Sampling locations .....	7
2.3 QA and QC in the field.....	9
2.4 Snow pits and physical parameters .....	9
2.5 Thawing of snow samples.....	12
2.6 Preparation of equipment for cleanroom .....	12
2.7 Preparation of NR solution .....	12
2.8 Filtration and staining of melted snow .....	13
2.9 QA and QC sampling and sample treatment .....	14
2.10 The method detection limit (MDL) .....	14
2.11 Visual analysis.....	15
2.12 Image analysis .....	15
2.13 Comparing manual and automated counting.....	16
2.14 Data frame and correction .....	16

2.14.1	Correcting for snow density.....	16
2.14.2	Calculating particle size.....	16
2.15	Statistical analysis and data processing .....	17
3	Development of protocol .....	18
3.1	Snow sampling.....	18
3.2	QA and QC in the field.....	18
3.3	Storage and handling of snow samples .....	19
3.4	Solvent and Nile red concentration .....	19
3.5	Stereomicroscope modification.....	19
3.6	Staining of plastic and possible artifacts .....	20
3.7	Establishing aliquot volume based on NR trials .....	21
3.8	Filtration and staining of samples .....	21
3.9	QA and QC in the laboratory .....	21
3.10	Counting of microplastics .....	22
4	Results.....	23
4.1	The occurrence of MP particles .....	23
4.2	The difference in MP sizes between urban and rural sampling sites .....	26
4.3	Viability of the method.....	28
4.3.1	Field blanks and MDL.....	28
4.3.2	Comparing manual count to automatic count.....	29
4.3.3	Background noise in images .....	30
5	Discussion .....	31
5.1	Method adaptation.....	32
5.1.1	Internal suitability of NR staining.....	32
5.1.2	Determination of the MP count.....	33
5.1.3	Comparability with other MP detection methods .....	33

5.2	Application of the method for the determination of MPs in snow.....	34
5.2.1	Amount of microplastics in rural and urban areas .....	34
5.2.2	Size classes of MP particles in urban and rural stations.....	36
5.3	Study conclusion .....	36
5.4	Perspective for future research and practice .....	37
6	Conclusion.....	38
	References.....	39
	Appendix A.....	I
	Appendix B .....	III
	Appendix C .....	XIII
	Appendix D.....	XIV



# 1 Introduction

Since the commercialization of plastic in the 1950s, its production has increased and is still increasing (Geyer et al., 2017). Plastics have a long lifetime and are reasonably resistant to use but are often found in products designed for one-time use. If plastic waste is mismanaged or lost, this long lifetime becomes a problematic property. Plastic pollution has gained widespread attention among the public because plastic litter is unaesthetic and has resulted in community responses, such as beach cleaning campaigns worldwide.

## 1.1 Plastic pollution- sources and size classes of particles

Plastics can be categorized into size classes, the four main classes being megaplastics (larger than 1m in size), macroplastics (1 m to 5 mm), microplastics (MP) (5 mm to 1  $\mu$ m) and nanoplastics (less than 1  $\mu$ m) (Ryan et al., 2019) (Figure 1). In this master thesis, the focus will be on the MP size range (5 mm to 1  $\mu$ m).

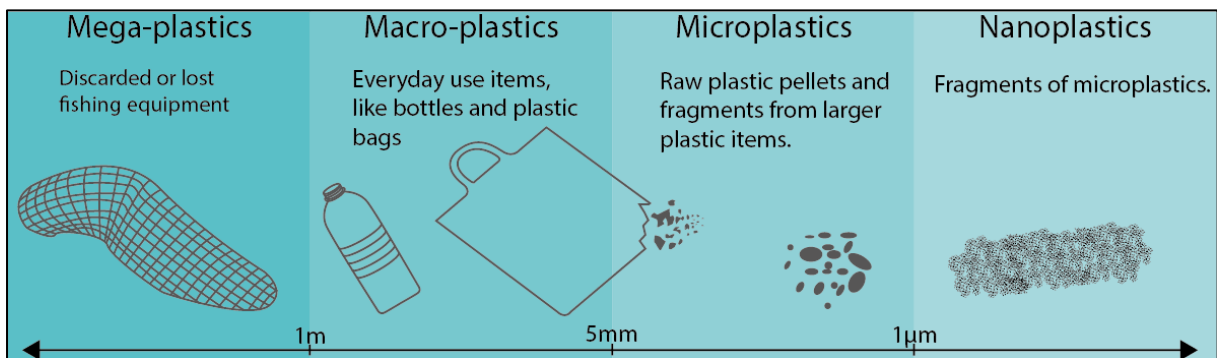


Figure 1: Size ranges of plastic debris defined in (Ryan et al., 2019).

Plastic pollution is exclusively of anthropogenic origin; to understand the sources of MP, an understanding of the sources of all sizes of plastic is necessary. Even though plastic pollution is mainly originating from terrestrial sources, the focus of research has mostly been on the marine environment. The spread of terrestrial plastic pollution is, therefore, largely unknown (Rillig, 2012). There is most certainly plastic pollution on land due to landfills, littering, and sewage (containing MP) used as fertilizer (Keller et al., 2020).

Over 80% of plastic pollution in the ocean has a terrestrial origin (Eunomia, 2016). One of the main sources is the littering of everyday items (Eunomia, 2016). The remaining plastic

pollution originates from sources at sea, like discarded or lost fishing gear, intentional and unintentional, loss of litter from fishing and shipping (Eunomia, 2016).

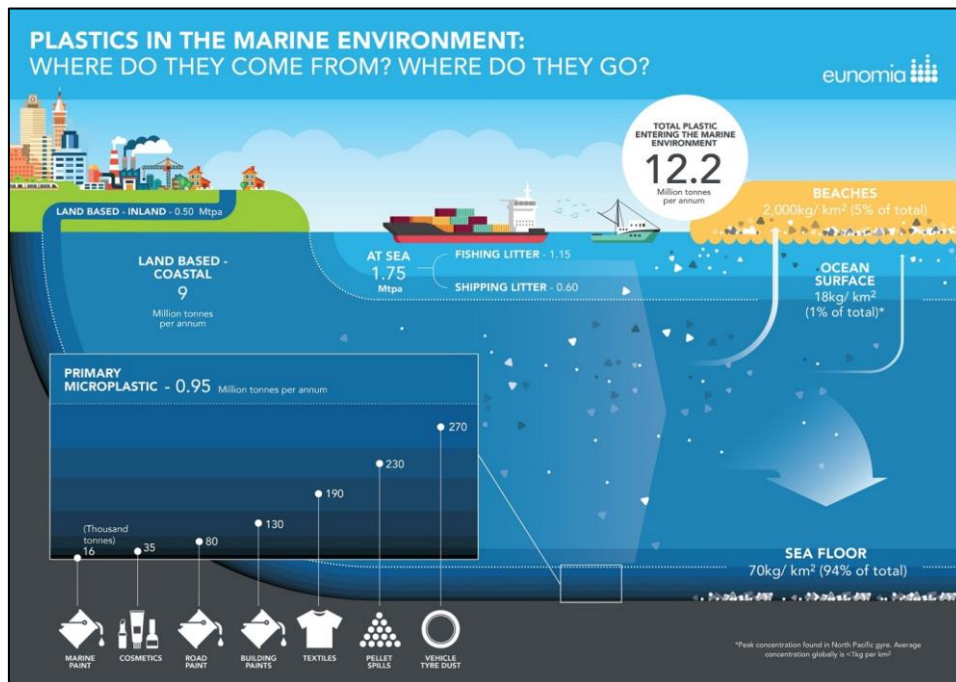


Figure 2: Sources of plastic pollution to the marine environment from (Eunomia, 2016).

The sources of MPs are, in many instances, tied to the source of macro- or megaplastics. To elucidate the sources of MPs, an understanding of the origin of larger plastics is necessary. MPs can originate from both primary and secondary sources. Primary MPs are particles that entered the environment in sizes smaller than 5mm. They are often emitted during production or use of plastic products such as personal care products (containing MPs), cosmetics, abraded MPS from car tires (Kole et al., 2017; Sommer et al., 2018), or lost from product manufacturing plants that use MP beads as a raw product (Sundt et al., 2014). The secondary source of MPs results from the breakdown of larger plastic items caused by environmental factors, such as ultraviolet radiation, hydrolysis, mechanical abrasion, and biological degradation (Andrady, 2011; Hepsø et al., 2018). In countries where waste management is poor, discarded plastic items reach the environment where they are eventually broken down. Subsequently, secondary MP pollution is highest in countries with insufficient waste management (Boucher & Friot, 2017). In the literature, fibers are often mentioned separately, although they also fit the category of MPs if they are synthetically produced. Fibers can be both primary or secondary MPs.



Several studies show that MP particles are ingested (intentionally and accidentally) by various marine organisms (Hall et al., 2015; Neves et al., 2015) and seabirds (Trevail et al., 2015). As MPs become ubiquitous in the environment, negative effects on organisms and human health are expected although not fully understood yet (Barboza et al., 2018).

## 1.2 Pathways

MPs can be found in almost all parts of the world, they have been found on the ocean floor, in all oceans, rivers, and estuaries (Yonkos et al., 2014), in sea ice and remote parts of the Arctic (Kanhai et al., 2020; Obbard et al., 2014). The pathways explored so far are mainly waterways, such as rivers and ocean currents. Plastic particles amass in oceanic gyres that are formed around the world because of large ocean currents (Eriksen et al., 2013; Maximenko et al., 2012). The ocean currents transport MPs from urban areas in the boreal and tropical regions up to the Arctic, spreading plastic into environments where there are only a few local sources of plastic pollution (Cózar et al., 2017; Eriksen et al., 2013).

Atmospheric deposition is a potential pathway for MPs that has been overlooked but has received increasing attention over the past years. Two types of atmospheric deposition are dry and wet. Dry deposition occurs when particles suspended in the atmosphere sink until they reach the ground. Wet deposition is when particles are caught by either rain or snow and, in that way get transported back to the ground. Snow physicists have long observed the wet deposition of particles by snow, also described as scavenging of particles (Browse et al., 2012). Several studies done on black carbon, for example, have been able to track particle pathways from forest fires in Canada to Greenland (Thomas et al., 2017). Based on observations of black carbon traveling large distances, it is questioned whether MPs are prone to undergoing a similar fate.

A previous study has investigated the presence of MPs in snow through the collection of snow samples from central Europe and the polar ice cap (Bergmann et al., 2019). Bergmann et al., (2019) found that there are MP particles in the snow on the polar ice cap and in remote areas on Svalbard and central Europe. The number of particles was reported per liter of meltwater. Central Europe had significantly higher numbers of particles ( $24.6 \pm 18.6 \times 10^3$  particles L<sup>-1</sup>) compared to the Arctic ( $1.76 \pm 1.58 \times 10^3$  particles L<sup>-1</sup>). The numbers for arctic snow were lower but still high when considering the remoteness of sampling locations.

Bergmann et al. (2019) is the first publication on MPs in snow; however, it is not the first publication on atmospheric deposition of MPs. Atmospheric fallout of MPs has been investigated before in France (Paris) and China. The collection of both wet and dry atmospheric depositions in more or less dense urban environments revealed the presence of microplastics in the form of synthetic fibers (Dris et al., 2016) They also found more synthetic fibers in the denser urban sites compared to the lower populated suburban environments (Dris et al., 2016). The latter study cannot exclude the input of synthetic fibers from the urban environment and, therefore, does not fully support the hypothesis of long-range transport (LRT).

In the high arctic regions, plastic sources are scarce and distant from each other. Large plastic pollution sources are human settlements and cities. The Arctic makes an ideal study environment for testing the LRT of MPs as it contrasts with more southern regions where pollution sources are numerous and closely spaced. While an increasing number of studies are currently being performed on MPs in the high Arctic, scientific data is scarce due to logistically challenging sampling conditions further hindering large-scale pan-Arctic studies.

The methodology of quantification and identification of MP in environmental samples is expensive and not standardized. A standard method should be applied to environmental samples to establish a holistic understanding of MPs in the environment while developing new methods. The most common method to identify and quantify MPs is by Fourier-transform infrared spectroscopy (FTIR) or Raman spectroscopy. Spectroscopy is automatic, however quite time consuming even for small samples volumes. Visual analysis of MP particles has also been a common method for the quantification and identification of MPs. Visual quantification is, however, suboptimal as plastic pieces that are transparent or white are easily overlooked while they could account for a large proportion of MPs in the environment. By manual counting particles that are not MPs can be falsely identified as MPs. Visual counting can therefore be inaccurate, and yield false positives (Lenz et al., 2015).

Nile Red (NR, 9-diethylamino-5-benzo[a]phenoxazinone) staining of MPs has shown promising in several studies as a quick approach to quantification in environmental samples. A standardized protocol for NR is lacking, but it has been used in several studies on sample

matrices such as sediment, seawater and laboratory test samples containing sand and MPs (Erni-Cassola et al., 2017; Maes et al., 2017; Shim et al., 2016).

### **1.3 Methodological limitations in MP research**

MP research is a growing field of science, and the methods are either lacking in efficiency, validation, or are costly, making research hard to reproduce around the world. In the absence of easy, cheap, and reproducible methodologies, studies are hard to compare, with many reporting concentrations of MP particles at different size scales and with different Quality Assurance (QA) and Quality Control (QC) regimes. Another issue impacting comparability is the reporting of results with different units. Moreover, the self-contamination of samples (i.e., MPs transferred from fieldworkers to collected samples) is an overlooked issue adding to discrepancies between studies.

### **1.4 Thesis description**

Snow sampling was done in the Tromsø region in northern Norway. Large amounts of snowfall for both 2019 and 2020 made sampling easy and accessible. Tromsø city and the surrounding area had many sampling sites suitable for snow profiles and snow collection. Furthermore, sampling in Tromsø and the surrounding area enabled the comparison between urban and rural snow.

In this master thesis, we investigated an inexpensive yet promising method, staining of organic materials with NR, to detect and quantify MPs in the snow. NR has originally been used to stain lipids in organisms, but it also stains plastic polymers. NR is a lipophilic stain that becomes fluorescent in combination with lipids/plastics. There have been several promising studies published recently, using NR to detect and count plastics (Erni-Cassola et al., 2017; Maes et al., 2017; Shim et al., 2016). Maes et al. (2017) managed to stain MPs in marine sediments while also testing NR with known plastic polymers. They found that spectroscopy identified the same particles as NR staining. Erni-Cassola et al. (2017) found that staining MPs with NR is a highly effective method to detect and quantify MPs in water column samples. Shim et al. (2016) tested NR on MPs under laboratory conditions, their conclusion was that NR works well for staining plastic polymers. Shim et al. (2016) disagreed with Erni-Cassola et al. (2017) and Maes et al. (2017) that NR is suitable for staining environmental samples. This was due to the chance of staining organic material present in

environmental samples (Shim et al., 2016). In Erni-Cassola et al. (2017) and Maes et al. (2017) low staining times avoided the co-staining of organic material, and itw as therefore still applicable to environmental samples.

We adapted this NR method to snow samples. We applied the new methodology on snow collected from rural and urban sites in a low-Arctic location in order to 1) establish a protocol for sampling and analysing, 2) test the protocol with field samples and 3) describe the amount and sizes of microplastics in snow in urban and rural areas.

## 2 Materials and methods

### 2.1 Sampling strategy

To investigate potential differences between urban and rural snowfall, 10 locations were sampled. The locations were selected based on local knowledge and opportunity, as the sampling sites needed to be sufficiently flat. Five urban samples, four rural samples, and one control sample were collected. The control sample was taken at a site where we expected low to no contamination. From each location, three subsamples were taken, totaling 15 urban subsamples, 12 rural subsamples, and three control subsamples. For each subsample, temperature stratigraphy was recorded in addition to bulk snow density and snow hardness. To account for intra-subsample variation due to particles not being homogeneously mixed in thawed snow, five aliquots of 100 ml each were filtered, stained, and analyzed (Figure 3).

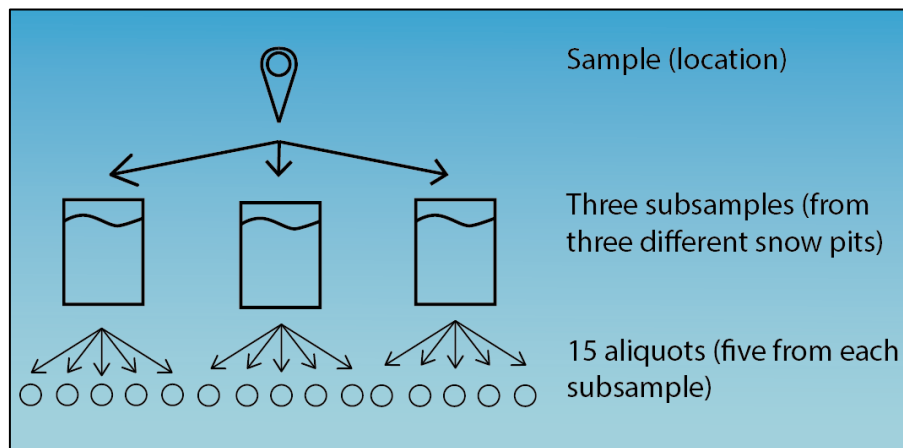


Figure 3: Diagram of the sampling approach. From each location, three subsamples were taken, each subsample was later split in 5 aliquots each.

### 2.2 Sampling locations

Snow samples were collected in northern Norway in the Troms county between 20<sup>th</sup> - 26<sup>th</sup> of March 2019. The only exception is the control sample, which was taken on the 7<sup>th</sup> of February 2020 (Table 1). Locations for snow sampling were split into two groups. The first group, “urban” (U1-U5) was within Tromsø city, with stations all located close to buildings and roads (Figure 4) and allowing the detection of potential local sources. The second group “rural” (R1-R4) was ~40km outside of the city away from buildings and with only one road close to the sampling sites (Figure 4), providing easy accessibility and sufficient flat and large open areas for sampling. The control location (station C) was at a higher altitude (487 masl) compared to the other stations, with a steep hill separating it from the city.

Table 1: Table of sampling locations, containing sample ID, location name, coordinates in decimal degrees (DDM), date, and group.

SAMPLE ID	LOCATION	LATITUDE (DD)	LONGITUDE (DD)	DATE	GROUP
U 1	Valhall	69.659759	18.955601	20.03.19	Urban
U 2	Meteorological institute	69.653406	18.936110	20.03.19	Urban
U 3	Kongsbakken park	69.649809	18.950792	21.03.19	Urban
U 4	Polaria bus stop	69.645411	18.948329	21.03.19	Urban
U 5	Mellomveien	69.638982	18.932134	21.03.19	Urban
R 1	Snarbyeidet	69.785515	19.541861	25.03.19	Rural
R 2	Snarbyeidet	69.766570	19.554537	26.03.19	Rural
R 3	Snarbyeidet	69.766564	19.563518	26.03.19	Rural
R 4	Snarbyeidet	69.775733	19.545537	26.03.19	Rural
C	Fløya	69.629380	18.990540	07.02.20	Control

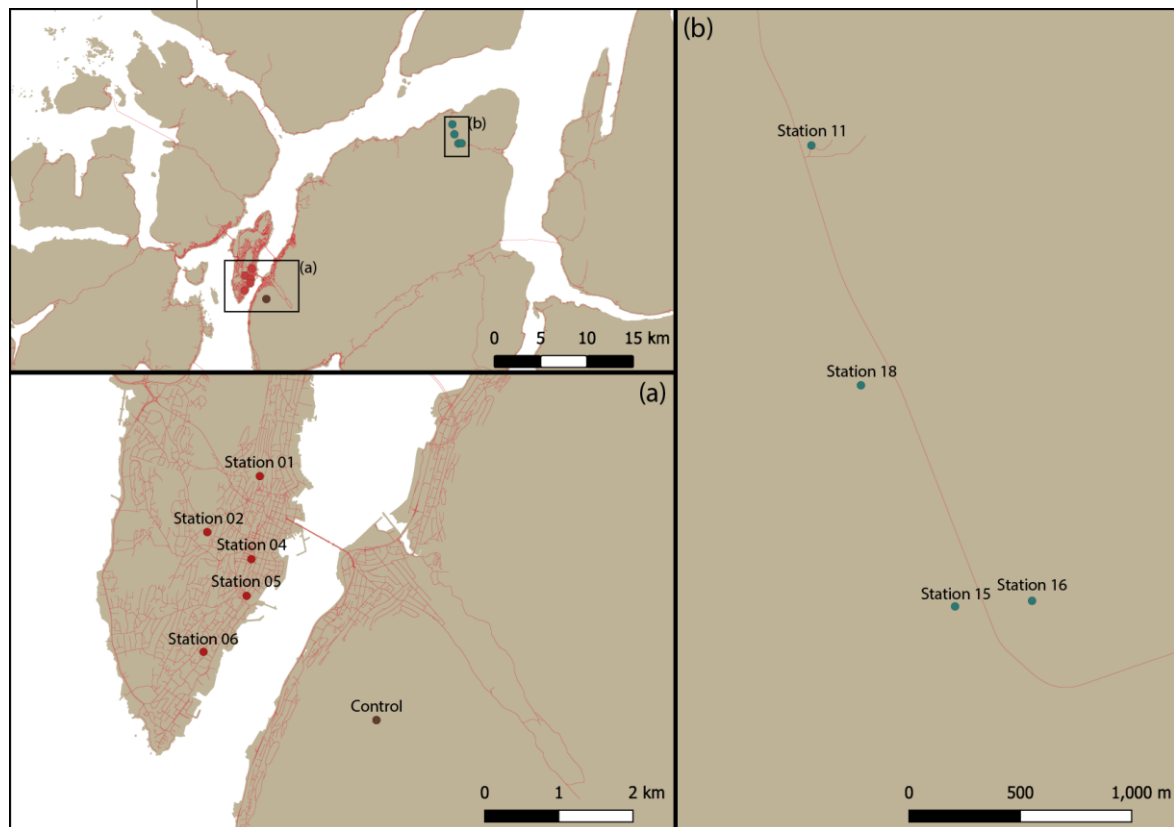


Figure 4: Overview of locations. (a.) Urban locations except for the control sample. (b.) Rural locations. The map was produced with QGIS (version 3.12.1) with map data from the Norwegian mapping and cadaster authority.

## 2.3 QA and QC in the field

During the sampling process, preventative measures were taken to minimize the contamination of samples. The equipment used for the collection of snow was made of metal. To keep the gear weight at its lowest, a Whirl Pak 550 (WP550) plastic bag was used as a sample container, although this is made of low-density polyethylene and could be a potential source of plastic in the samples. Moreover, as many outdoor clothes are made of synthetic materials, we could not entirely exclude the risk of contamination. For each sampling day, we took a photo of the people performing the sampling (Figure 5). One blank sample was done at each location, to get an estimate of contamination occurring during sampling. The blank sample was obtained by leaving one sampling bag open during a sampling procedure, handling it similar to a true sample, though without snow.



*Figure 5: Example of clothes worn by person performing snow sampling.*

## 2.4 Snow pits and physical parameters

Sampling was performed following Gallet et al., (2018) with minor adaptations. In brief, snow pits were oriented towards the wind so that any snow excavated would not blow back into the pit. If there was no wind, the snow pit was oriented towards the sun so that the sampling wall was in the shade. The snow was excavated until the snowpit reached the bottom ice layer or around 5-10 centimeters above the ground. At each location, three snow pits were excavated as subsamples (~2 m apart) to account for local variability. For each of the pits, snow density was measured.

Snow density measurements were performed in one column from the surface (top) to the bottom. Density measurements were recorded with a steel cutter tube with a volume of 0.5 L, a length of 26 centimeters, and a weight of 536 grams. The tube was pushed down from the top and extracted with the snow inside then weighed on a scale (resolution of 0.1 gram). If hard layers made the procedure difficult, a soft hammer was used to push the tube through. Figure 6 shows the equipment used to collect snow density measurements.



Figure 6: Equipment used for measurement of snow density.

Snow hardness was tested throughout the snow column using a simple hand test, as described in Fierz et al. (2009). The hand test allowed for a quick overview of the softer and harder layers on the sample wall. On the shaded wall in the snow pit, the temperature was measured every 5 centimeters with a VWR Calibrated Electronic Thermometer with Stainless Steel Probe. Snow depth was measured at each site using an avalanche probe (Mammut probe 240). Across the sampling locations, snow depth varied between 70 to 100 centimeters (Table 2). Therefore, to make sure to collect an even amount of snow, small parts of the snow column were gradually transferred into the WP550 bag using a metal shovel or a metal spatula until the bag was full. To make sure that there would be enough meltwater in case particle loads were low, 2-3 liters of snow were collected. Snow samples were stored in freezing rooms and because of space limitations, some samples were stored at  $-5^{\circ}\text{C}$  and others at  $-20^{\circ}\text{C}$ .



Table 2: Overview of snow depth at each sampling location.

<b>STATION</b>	<b>SNOW DEPTH</b>
<b>U1</b>	70 cm
<b>U2</b>	90 cm
<b>U3</b>	90 cm
<b>U4</b>	70 cm
<b>U5</b>	100 cm
<b>R1</b>	70 cm
<b>R2</b>	80 cm
<b>R3</b>	70 cm
<b>R4</b>	70 cm
<b>CONTROL</b>	70 cm

## **2.5 Thawing of snow samples**

Snow samples were taken out of the cold rooms at least 24 hours before the laboratory procedure. During transport and thawing, the samples were handled with care so that no mechanical stress would act on the bags. Samples that were kept at -20°C were double bagged to preserve sample material due to higher prevalence of leaking.

## **2.6 Preparation of equipment for cleanroom**

All handling of the thawed snow samples was done in the cleanroom located at the Institute for Air Research (NILU), Tromsø. The equipment used for the filtration and staining procedures had to be cleaned for all plastic particles. All glass and metal wares were washed, covered in tinfoil, and burned at 500°C for 8 hours one day before use. To use the cleanroom at NILU Tromsø, there was a strict chemical-free regime; this meant no use of cosmetic products or soaps for 12 hours before entering the cleanroom. In the cleanroom, a synthetic overall always had to be worn, in addition to boots and hood. The latter precautions were not to prevent plastic contamination, but chemical contamination for other ongoing research. During the sample processing, no gloves were worn to limit direct contact of synthetic polymers.

## **2.7 Preparation of NR solution**

NR solution was prepared in the cleanroom by dissolving a technical grade NR powder (N3013, Sigma Aldrich) in 98% ethanol solution to obtain a concentration of 10 mg/L. The NR solution was filtered through a Whatman 47mm GFF filter (WHA1825047, Sigma Aldrich) to remove any plastic particles before transferring to the pre-burned glass container and then covered with tin foil.

## 2.8 Filtration and staining of melted snow

The filtration equipment consisted of a 2 liter Erlenmeyer flask, a filtration head with a connection for the vacuum pump to be used with 47 mm filters, and a 500 ml funnel (Figure 7). Three complete sets were used simultaneously to process one location (i.e., three sub-samples) in one day. In order to avoid cross-contamination between subsamples, each subsample was filtered with the same column. One hundred ml of meltwater was filtered and pumped dry before releasing the vacuum by disconnecting the pump tube. The funnel wall was rinsed with filtered water to remove any particles adhering to it. With a glass pipette, ~2 ml NR solution was applied, so that it covered the filter entirely with a thin layer and was left to stain for five minutes. The pump was connected to remove any excess NR in the filters. The filter was rinsed with 50-100 ml of filtered water to remove any remaining NR on the filter, as this would show up during the visual analysis. The funnel wall was thoroughly rinsed to make sure no plastic particles remained on the equipment.



Figure 7: Filtration setup used for filtering and staining of samples.

When all aliquots (3x5) of a location had been processed, the field blank WP550 bags were filled with 500 ml of filtered water, shaken vigorously, and then processed following the same procedure as described. To get an estimate of the possible contamination generated by the laboratory process, 100 ml of filtered water was filtered and stained. After the filtering and staining processes were completed, the filters could be removed from the cleanroom as additional contamination would no longer be detected on the visual analysis.

## 2.9 QA and QC sampling and sample treatment

To get an estimate of how many particles were added to the samples during handling in the lab, as well as in the field, two different blank samples were taken throughout the sample handling period: 1) field blank and 2) lab blank. For each sampling location, one open bag was placed close to where the sampling was occurring. This field blank was then treated in the same way as the regular samples. During the laboratory procedure, one filter was treated the same way as the other samples but replacing melted snow with filtered water. However, as the contamination in the lab also would be incorporated into the field blanks (handled identically to a sample in the lab), the laboratory blanks were used to assess the magnitude of contamination during the handling in the lab. The lab blanks were not used to calculate a method detection limit (MDL).

## 2.10 The method detection limit (MDL)

The method detection limit is an approach to identify method threshold limits. The MDL was subtracted from each aliquot in the data. This removes the number of particles added by the sample collection and processing. The MDL was calculated using Equation 1

$$MDL = 3 * Standard\ deviation\ (blank\ samples) + mean(blank\ samples)$$

*Equation 1: Equation to calculate the method detection limit (MDL).*

The MDL was subsequently subtracted from the number of each aliquot. The MDL was, in some cases, higher than the number of particles recorded for a subsample leading to negative values for some subsamples. All values below the MDL were therefore set to zero.

## 2.11 Visual analysis

The filter with stained particles was placed under a Leica M-50 with an MC190 camera attached to it. A 3D printed filter holder containing eight blue LEDs and an orange filter were attached to the stereomicroscope. The LEDs would emit light waves at 470 nanometers exciting the NR. The light emitted from the NR stained particles would pass through the orange filter, while blue light was filtered out (Figure 8). This allowed us to take pictures of the filters with only the stained particles visible. Pictures were taken at a resolution of 2596x1944 pixels (~5 megapixels) with a 0.63 times magnification. The magnification of the stereomicroscope prevented the opportunity of taking one picture of the complete filter. Therefore, four pictures were taken through a grid and later cropped down so that each picture included one-fourth of a filter.

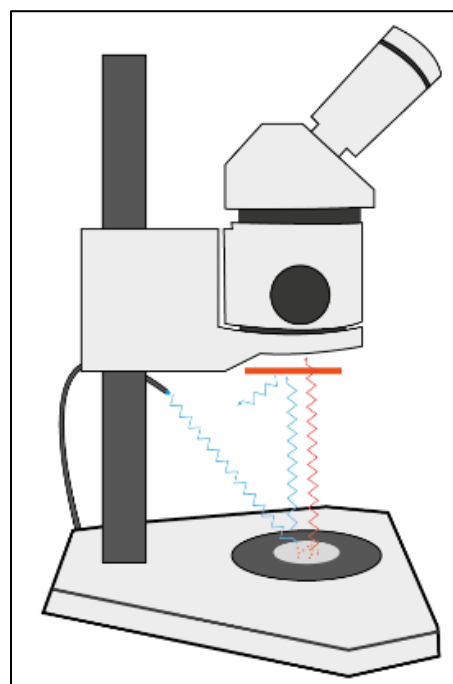


Figure 8: Schematic of stereomicroscope and light waves.

## 2.12 Image analysis

To standardize the way particles were counted and to decrease human error, the image software ImageJ (version 1.52) was used. ImageJ allows to set a threshold based on the light intensity; this was in our case set to 100 (out of 255) to exclude all dimly lit particles. In addition to the threshold, only particles that measured more than 3 pixels were recorded. All images were converted into black and white in Adobe Lightroom to use ImageJ for the count of particles. Adobe Lightroom also allowed for removing light specks that appeared outside the filter area. To count MPs from multiple images in sequence, a macro was written in ImageJ that allowed counting all images in each folder containing images from each location.

For each location, 84 images were analyzed using ImageJ that provided both the number of particles but also their largest diameter measured in pixels.

## 2.13 Comparing manual and automated counting

Randomly selected filters were counted manually and compared to the count obtained by ImageJ. Counting was done using the multi-point tool in ImageJ, allowing for click counting on the images taken through the Leica stereomicroscope.

## 2.14 Data frame and correction

The ImageJ macro (Appendix C) exported one excel file per picture with the number of particles and the area for each picture; these were imported to R (Version 3.4.4) and combined for each filter using the dplyr library.

### 2.14.1 Correcting for snow density

To be able to compare all stations, they had to be corrected for snow density. Snow density was calculated using Equation 2.

$$\text{Snow density}(g.L^{-1}) = \frac{\text{weight of tube with snow}(g) - \text{weight of empty tube}(g)}{\text{volume of tube}(L)}$$

*Equation 2: calculation is done to get the snow density in grams per liter.*

For each sampling location, three density samples were taken to get a more accurate snow density measurement. These three samples were averaged.

The average density was then used to calculate a correction factor using Equation 3. The density correction factor was calculated for each station.

$$\text{Density correction factor} = \frac{\text{snow ml}}{\text{volume L}} * \frac{n \text{ particles}}{100\text{ml}} = \frac{(n \text{ particles})}{L}$$

*Equation 3: Calculation of the multiplying factor to correct each station for snow density to get particles/L snow.*

### 2.14.2 Calculating particle size

ImageJ offers several methods to measure the size of particles, where the most commonly used is the area in pixels. Using a measurement function called Feret's diameter, the longest diameter could be measured. The value for diameter was given in pixels and transformed into micrometer using the software LAS EZ (Leica microsystems) while taking the magnification into account. We calculated the length of one pixel to be 11.47 $\mu\text{m}$  at the used magnification.

## 2.15 Statistical analysis and data processing

The automated count exported the values from each image into one .CSV file. As each complete filter consisted of four images they needed to be combined in to one file. Using the lapply and dplyr library in R, all files were merged in to one file per filter. The merged files contained information about the length of each particle, and the length of the file itself was the number of particles. The number of MPs were all transferred into one .CSV file, while all the measured sizes were transferred into another.

The numbers presented in the results and discussion are means  $\pm$  standard deviation (SD).

All graphical plotting and statistics were performed in R (version 3.4.4) with no additional packages. Exported plots were edited with Adobe Illustrator to enhance figures graphically.

The statistical comparisons between urban and rural stations were performed with a nonparametric Mann-Whitney U test. The test was selected based on the fact that the data was not normally distributed (Kolmogorov Smirnov test,  $D = 0.33968$ ,  $p > 0.001$ ). The Mann-Whitney U test was performed for the comparison of the amounts of particles between locations, to test if there was a significant difference in means. The mean of the standard deviations between subsamples was also compared with a Mann-Whitney U test.

The final working dataset was made up of 125 filters that were used for analysis (Figure 9).

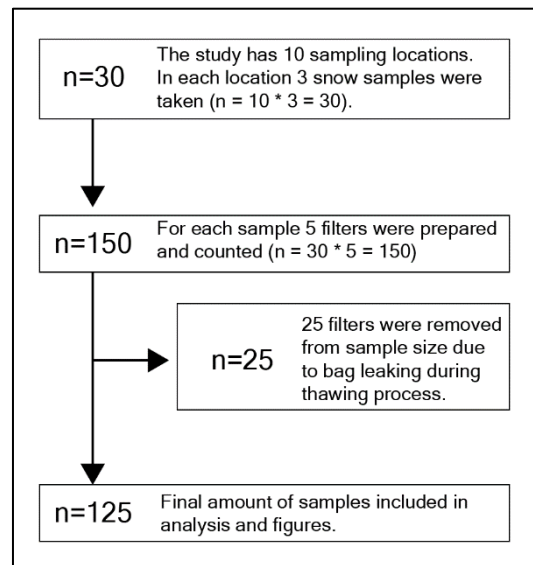


Figure 9: Overview of the final data set and the filters and why some were excluded.

### **3 Development of protocol**

The main aim of this thesis was to develop and test a method to sample, identify, and quantify MPs in snow. For this purpose, a protocol was established describing each step from sample collection, recording, and measuring essential parameters to QA, laboratory process, analyzation, and quantification. None of the techniques used in the protocol are new, but rather a collection of tested methods combined. The protocol serves as an effort to providing standardized methods, with an emphasis that it could be easily adapted to other environmental media and easy to reproduce. The protocol is attached in Appendix B.

#### **3.1 Snow sampling**

Our snow sampling protocol was based on (Gallet et al., 2018), with many elements simplified or removed. Following personal advice by J-C Gallet the snow physical properties recorded were density, depth, hardness, and temperature. All tools to record the listed parameters were available to purchase within a short time, except for a snow density tool. J-C Gallet provided a cutter tube with a known volume and weight for density measurements. Following an assumption that there would be low amounts of microplastics in the snow, a large sample container would be required. In (Gallet et al., 2018), a WP550 bag was used to collect snow samples for environmental carbon; as this was light and robust, it was ideally suited to our purpose. The drawback with WP550 bag is that it was made of high-density polyethylene, which could be a potential contamination source that had to be accounted for. Most equipment described in (Gallet et al., 2018) did not contain any or low amount of plastic parts. The foldable plastic ruler described in the protocol was replaced by an avalanche probe (Mammut probe 240).

#### **3.2 QA and QC in the field**

The most critical QA measure in the field was the field blank samples. The field blanks provide an estimate on how much plastic contamination is due to the sampling process (i.e., particles from the container, handling, or the equipment used in sampling). Also, to assess potential local contamination sources, each site was photographed, and any proximity to plastic sources was reported. The blank samples are used to calculate an MDL which is subtracted from the number of particles, ensuring that MPs present in the environment are counted.



### **3.3 Storage and handling of snow samples**

Since samples were collected and treated months apart, they had to be stored. Most samples were stored in a cold room (-5°C), but due to space limitations, some samples were stored in a freezer (-20°C). Samples stored in the freezer tended to leak when thawed, most likely due to the formation of hard ice crystals perforating the sampling containers. Before being processed and stained, all samples were thawed at room temperature for 24 hours. While thawing, sample containers were placed in buckets to prevent them from tipping over and spilling. Since contamination from the air could be an issue, all samples were kept closed during transport and thawing. Based on our experience from the different storage temperatures, we advise to store samples in a cold room at -5°C and to thaw samples with care.

### **3.4 Solvent and Nile red concentration**

When reviewing the literature, different solvents and concentrations were reported (Erni-Cassola et al., 2017; Maes et al., 2017; Shim et al., 2016). The most suitable solvent was ethanol, whose use is associated with lower health risks. The concentration that was tested and finally used was 10 mg/L. Although lower concentrations of NR have been reported as successful, a cautionary approach was taken, and a slightly higher concentration of NR used.

### **3.5 Stereomicroscope modification**

NR needs light waves between 450-510 nm to become fluorescent; this corresponds to the blue to the green light spectrum. Most stereomicroscopes are not provided with an option with light exclusively in that spectrum. To make a cost-effective option that did not require any specialized orders, a microscope attachment was made with eight blue LEDs. The LEDs were wired in parallel with a 33  $\Omega$  resistor each attached so they would not burn out. Using a USB cable, they could be attached to a 5 V power source (Appendix Figure D1). To see the emitted light from the NR, all the blue light needed to be filtered out. A deep orange filter film (Eurolite, 158 deep orange) intended for theatre lights was used to filter out all the light except for orange. Two layers of the filter film were needed to remove all blue light. The first experimental stereomicroscope attachment was made entirely out of cardboard and hot glue; a later 3D printed design was made by Jan Are Jacobsen at Norwegian Polar Institute. The 3D printed version is available and attaches to all stereomicroscope with a Leica M-series 1.0x Plan Objective. In addition, it is crucial to consider the background on which the filter will be

photographed. Black backgrounds worked best as they reduced light reflection and scattering, reducing image noise.

### 3.6 Staining of plastic and possible artifacts

The only filters available for the initial trials of NR were cellulose acetate filters. When staining particles on the filter, the filter itself was stained. Following the literature Whatman 47mm GFF filters were used, these filters are made of borosilicate glass fiber and were not stained by NR. Known polymers (Table 3) were stained to test the accuracy of the NR. All polymers tested except for rubber were stained by NR.

Table 3: Overview of polymers and potential artifacts stained with NR.

<b>POLYMER TESTED</b>	<b>SIZE OF PARTICLES</b>	<b>STAINED BY NR</b>
<b>PA</b>	50µm	Yes
<b>PE</b>	Pellets	Yes
<b>UPVC</b>	350µm	Yes
<b>PS</b>	250µm	Yes
<b>RUBBER</b>	Granulate	No
<b>LEAVES</b> (BIRCH, BETULA SP.)	Cut in small sections	No
<b>BARK</b> (BIRCH, BETULA SP.)	Cut in small sections	No
<b>GRASS</b>	Cut in small sections	No
<b>CELLULOSE</b>	NA	Yes (faint light)

Since NR is commonly used for staining organic material, we also stained biological material that is expected to be present in the snow. Namely, leaves, bark, and grass collected at sites were stained using the same method as for known polymers. Toilet paper that contains cellulose was dissolved in water and stained with NR. None of these items were stained by NR except for toilet paper. The cellulose in toilet paper showed a faint light under analysis; in comparison to plastic particles, it was barely visible.

### **3.7 Establishing aliquot volume based on NR trials**

One sample of ~5 L snow melted into 2-3 L of meltwater depending on density. Filtering the whole sample would have led to an overload of particles on the filter. We also assumed that the plastic particles within the sample were not uniformly distributed and that there should be high variability between aliquots. Therefore, we processed, stained, and analyzed aliquots of 50, 100, 150, 200, 300, and 500 ml. Based on the number and layering of particles, 100 ml aliquots were selected. Following the assumption of high variability within the samples due to low homogeneity, we decided to analyze five aliquots of 100 ml from each subsample.

### **3.8 Filtration and staining of samples**

Each of the three subsamples in a sample were processed using a different filtration set to avoid cross-contamination between subsamples. The walls of the funnels were rinsed with filtered tap water (pore size: 0.7  $\mu\text{m}$ ) to make sure all particles were washed down on the filter. The most convenient and efficient way to stain the samples was to leave the filter in the filtration setup and add the Nile Red solution onto the filter. This limited the handling of filters. During initial trials of staining with NR, we found out that the vacuum pump had to be disconnected when adding NR in order not to get sucked through the filter but remain on the filter. The NR solution was left on the filter for 5 minutes to stain. The vacuum pump was then reconnected, and the solution and filter were washed with prefiltered tap water to remove any leftover NR. After the samples were filtered, stained, and rinsed, they could safely be taken out of the cleanroom as they needed to be analyzed in a dark room.

### **3.9 QA and QC in the laboratory**

Our method was performed in a cleanroom (NILU, Tromsø) to ensure minimal contamination during the laboratory procedure. Most parts of the filtration equipment were made of glass or metal. The major plastic equipment used in the laboratory procedure was the vacuum pump and hose, but neither of them was in direct contact with the samples. The equipment and filters were burned at 500°C for 8 hours before use to remove any residual microplastic particles on it. Smaller equipment was packed in tin foil and openings of glass equipment covered with tin foil. Procedural blanks, to estimate the plastic contribution from the laboratory process, were obtained by processing filtered water in the same way as snow samples using a clean filtration set.

### 3.10 Counting of microplastics

In order to capture the whole filter with the microscope camera, we took four images using a grid drawn on a glass petri dish placed on top of the filter (Figure 10). Each image was cropped down to each quadrant so that no part of the filter overlapped. When examining the test samples, it appeared that the manual count of particles was time-

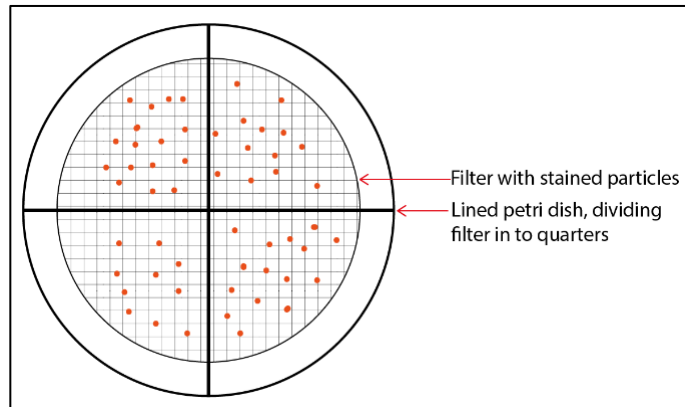


Figure 10: Schematic of how filters were photographed in quarters with the use of a lined petri dish.

consuming since each filter displayed up to hundreds of particles. As an alternative, we explored ways of automatic counting. We first created a script in R using the EBImage library. The EBImage library was initially intended for the counting of nuclei in cells; it was unpractical to adapt this method for counting microplastic particles. (Erni-Cassola et al., 2017) reported the use of the software ImageJ which proved to be a better tool for counting plastic particles. We, therefore, wrote a macro in ImageJ (using basic JavaScript) that allowed not only the count of particles but also produced output information about the individual particles such as their longest diameter and area in pixels. Using the software supplied with the Stereomicroscope (Leica Application Suit X, Leica microsystems), the length of one pixel in  $\mu\text{m}$  at the used magnification could be calculated. The combination of microscope photography and the software ImageJ enabled the count of particles and measurement of their sizes.

Thirty randomly selected filters were counted both manually and automated, to validate the automated count. The manual count assured that the count from ImageJ did not overestimate the number of plastic particles and could, therefore, be used for counting of MPs.

## 4 Results

### 4.1 The occurrence of MP particles

The MDL calculated was 184 particles  $100 \text{ ml}^{-1}$ ; it was subtracted from each aliquot. It was ensuring that the number of particles reported did not include contamination from the sampling and/or laboratory procedure. The mean number of particles in the urban samples was  $681 \pm 375$  particles  $\text{L}^{-1}$  of snow, while the mean in the rural sites was  $439 \pm 286$  particles  $\text{L}^{-1}$  of snow. The number of particles was significantly different between urban and rural locations (Mann Whitney U-test, U-value=2227,  $P < 0.0001$ ), being twice as high in the urban areas compared to the rural areas (Figure 11).

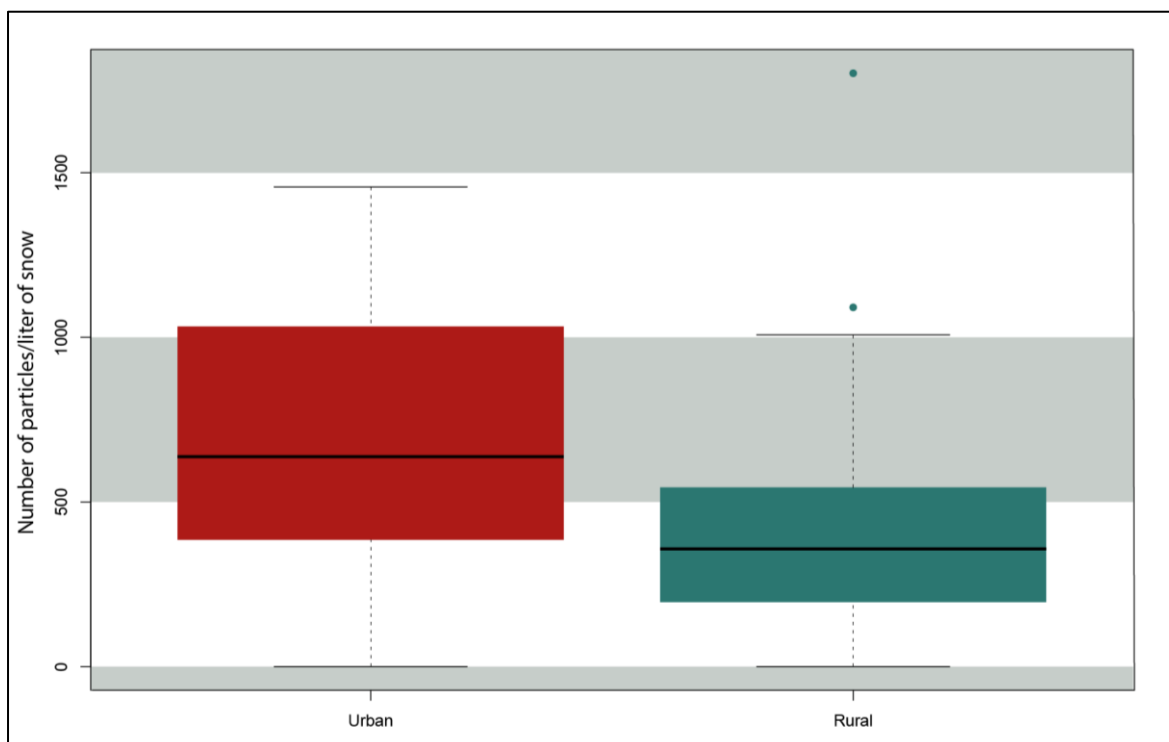


Figure 11: Boxplot over the number of particles  $\text{L}^{-1}$  snow in all the urban locations (red) and all rural locations (green).

Nevertheless, it is noteworthy that one rural location (R01) showed a higher mean of particles ( $815 \pm 136$  particles  $L^{-1}$ ) compared to the other rural locations ( $323 \pm 40$  particles  $L^{-1}$ ) (Figure 12).

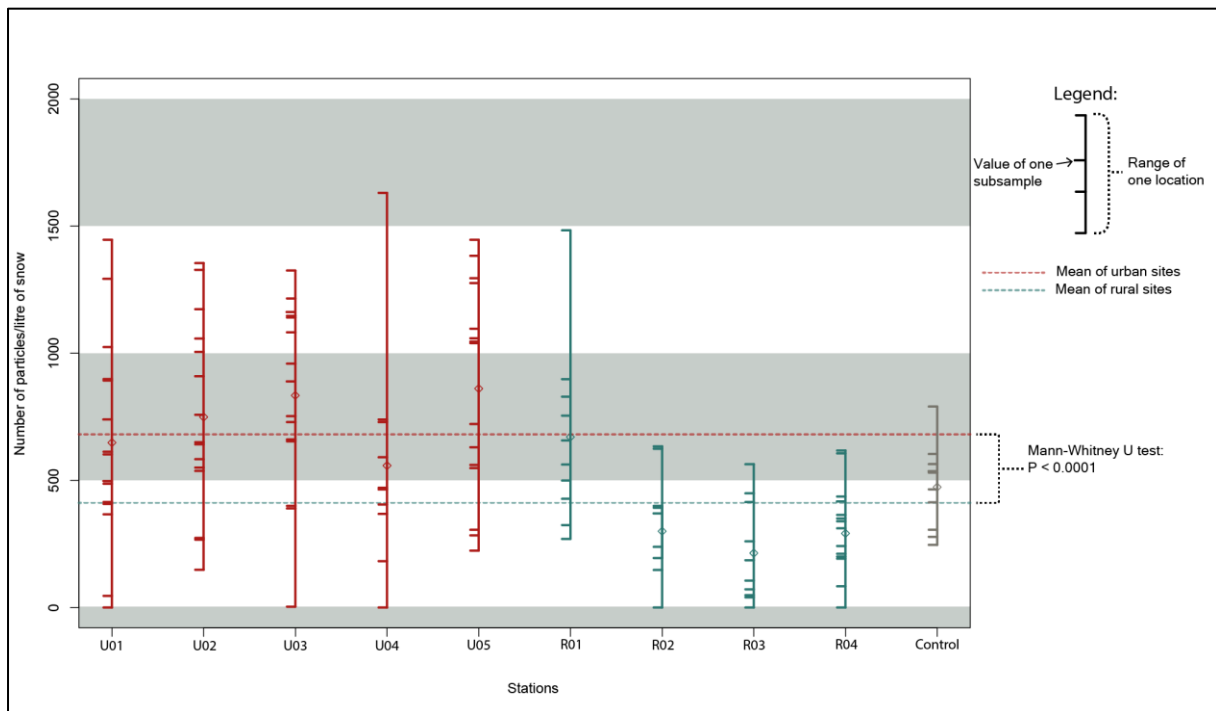


Figure 12: Number of particles per liter of snow for each station. Red lines (U1-U5) represent the urban samples, the green lines (R1-R4) represent the rural locations and the grey lines (Control) represent the control sample. Mann-Whitney U-test gave a significant difference,  $P < 0.0001$ .

The standard deviation for the urban stations was significantly higher than the standard deviation for the rural stations (Figure 13). The average standard deviation was 25% higher for urban stations compared to rural stations (375 vs. 286, respectively). The lowest variation was in the control sample, indicating that the sample was more homogenous at the control site than at any of the other sites. The standard deviation was 55% of mean number MPs in urban locations, while in the rural stations, it was 65% of mean number MPs.

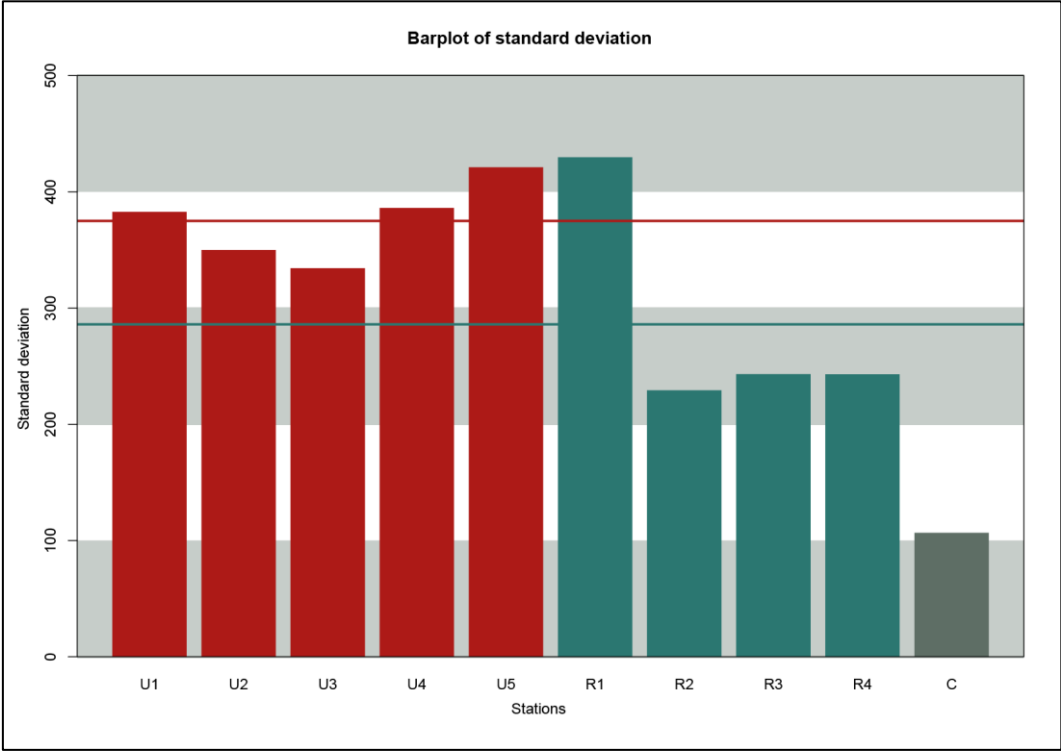


Figure 13: Bar plot of the standard deviation for each sampling location. Blue-green bars represent the urban locations; red represents rural locations; grey represents the control location. The red horizontal line represents the mean of the standard deviation in the urban locations, while the blue-green shows the mean of the standard deviation for the rural stations.

## **4.2 The difference in MP sizes between urban and rural sampling sites**

The combination of the 0.63 times magnification and the 5-megapixel camera resolution, the smallest length that could be recorded, was 22  $\mu\text{m}$  in diameter. The longest length of particle found in this study was 7983 $\mu\text{m}$ .

For both urban and rural stations, the most abundant MP particles were smaller than 200  $\mu\text{m}$  in diameter (Figure 14). The distribution of the smaller sizes differed when comparing urban to rural areas. The rural stations had a higher proportion of the smallest size class (22-50  $\mu\text{m}$ ) (45.5% vs. 38.6%); for all classes up to 200  $\mu\text{m}$ , the urban stations had a slightly higher proportion of MPs ranging from 2.5 % to a 0.2% difference. Overall, the mean of the urban stations was 82.34  $\mu\text{m}$  compared to 79.27 $\mu\text{m}$  for the rural stations (Mann Whitney U test,  $W=20977000$ ,  $p>0.0001$ ) for all particles. MPs were grouped into size classes starting from 22-500  $\mu\text{m}$  or more; the grouping was in 25  $\mu\text{m}$  increments; the only exceptions were the smallest and largest size class. The rural stations had a higher proportion of the total amount in the smallest size class.



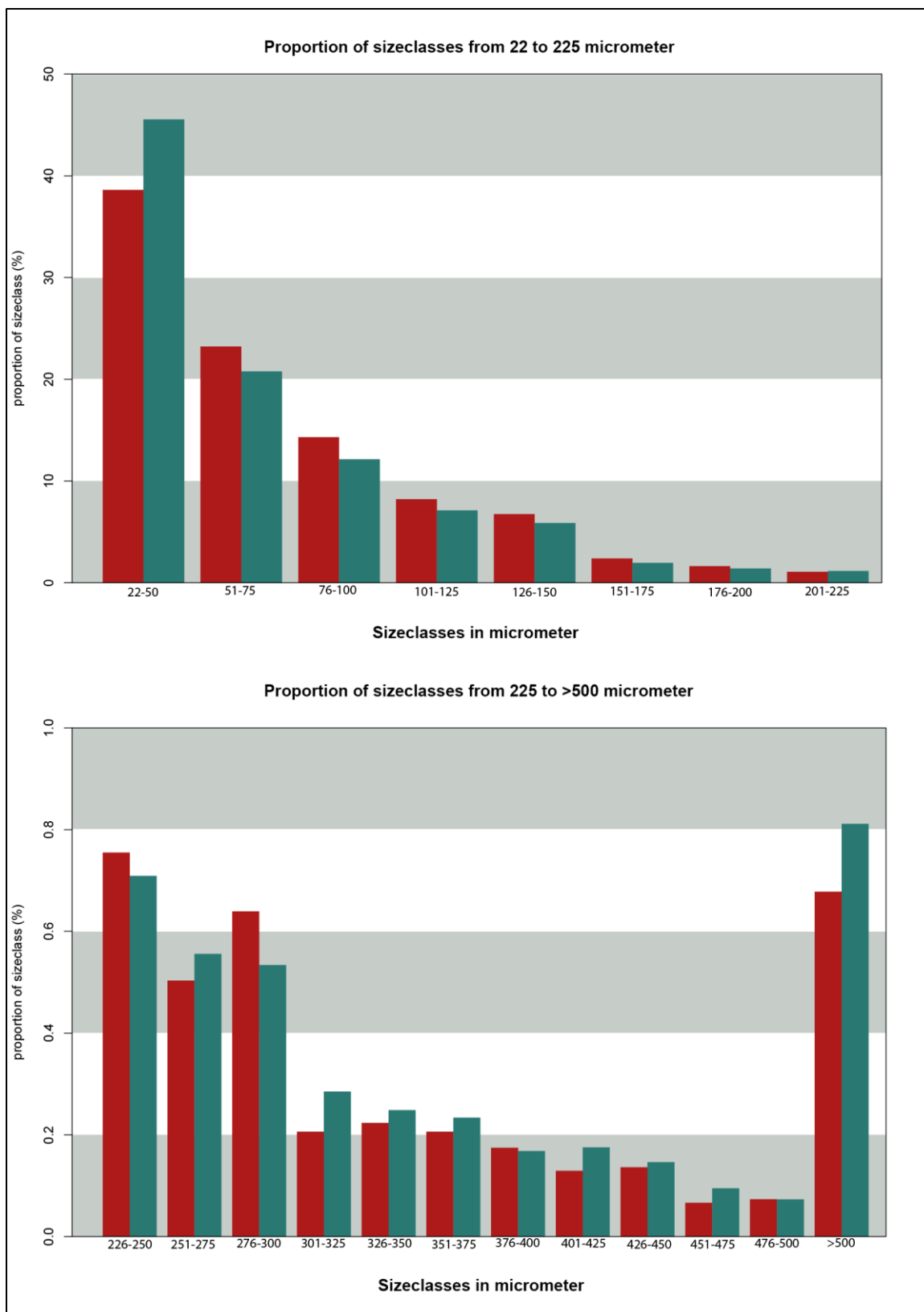


Figure 14: Proportion of each size class MP particles, the red bars represents the proportion of urban size classes, and the blue-green bars represent the proportion of rural size classes. (top) Size classes from 22-225  $\mu\text{m}$ , and y-axis from 0-50%. (bottom) Size classes from 225 to >500, with y-axis 0-1%.

## 4.3 Viability of the method

### 4.3.1 Field blanks and MDL

The field blanks were all counted and calculated into the MDL. In Figure 15, the boxplot illustrates the recorded aliquots from each field blank. The blue line in Figure 15 illustrates the calculated MDL. None of the field blanks were higher than the MDL. The average number of MPs in the field blanks was 67.3 particles 100 ml<sup>-1</sup>, while the standard deviation was 39.6 particles 100 ml<sup>-1</sup>. Because the field blanks were treated in the laboratory process, contamination from the laboratory process is already incorporated into the field blanks. Therefore, the number of MPs in the lab blanks was not subtracted from the dataset but served to illustrate the amount of laboratory contamination. The average of particles found in lab blanks was 20.4 particles 100 ml<sup>-1</sup>, amounting to approximately a third of the MPs found in the field blanks (Figure 16). Subtracting the lab blanks from the field blanks gives on average 46.9 particles 100 ml<sup>-1</sup>, which is the average contribution of contamination from field sampling.

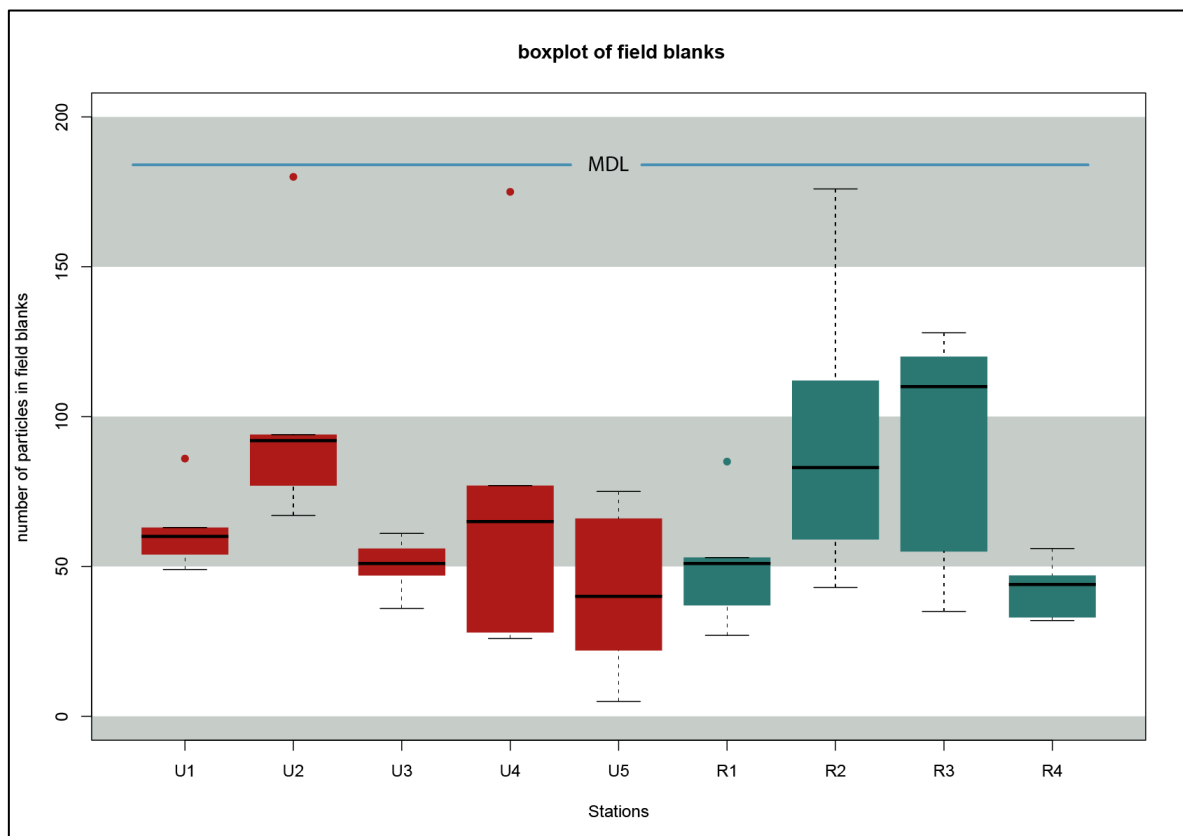


Figure 15: Boxplot of field blanks, the red bars represent urban locations, blue-green bars represent rural locations. The blue line represents the MDL.

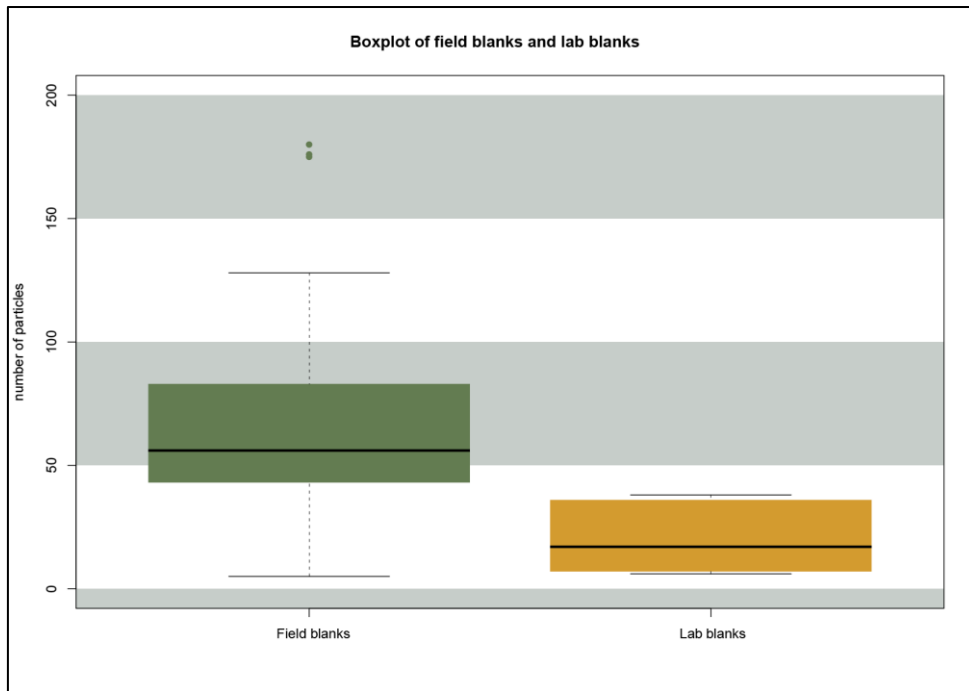


Figure 16: Boxplot comparing the number of counted MPs in field blanks and lab blanks. The green box is for the field blanks, the yellow box is for the lab blanks.

### 4.3.2 Comparing manual count to automatic count

For all samples, the manual count was significantly higher than the automatic count (Mann Whitney U test,  $W = 734.5$ ,  $P < 0.0001$ ) (Figure 17) with a mean of 187 particles for the manual count vs. 87 particles for the automatic count.

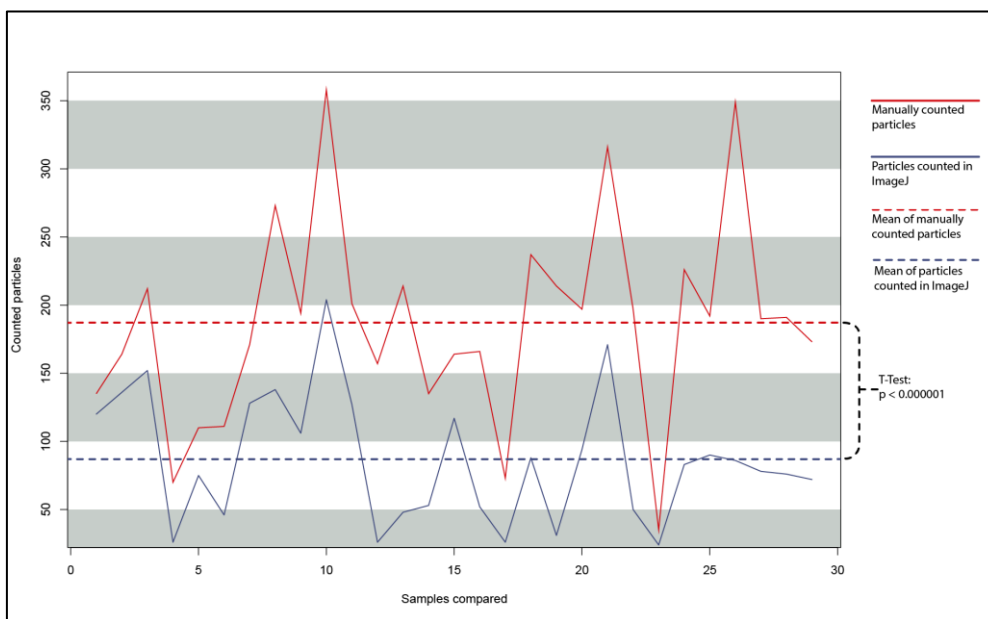
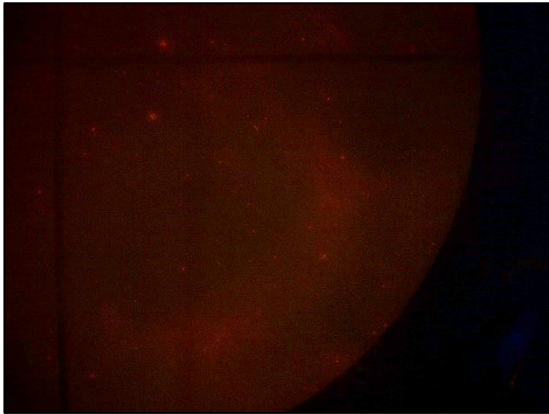


Figure 17: Comparison between manually counted and automatically counted particles in the same pictures.

### 4.3.3 Background noise in images

For some filters, the remains of NR created background noise that was observed more often in blank samples (Figure 19) or samples with few MP particles (Figure 18). The background noise was partially removed in Adobe lightroom by increasing contrast and decreasing exposure. However, we are confident that the background noise did not influence the count as particles were still distinguishable (Figure 18).



*Figure 19: One quarter filter from a blank sample in R01. Background noise is visible as red “clouds” due to lack of contrasting particles. Light and contrast increased for viewing purposes.*

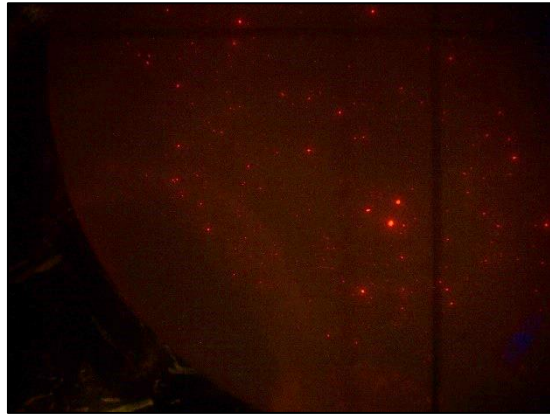


*Figure 18: One quarter filter from a sample in R01. Background noise not visible in the same manner as contrasting particles are present. Light and contrast increased for viewing purposes.*

## 5 Discussion

In recent years, MPs have been found in most natural media explored, highlighting the importance of monitoring its presence. Confirming the presence of MPs in snow is essential to understand alternative transport mechanisms across landmasses and from land to the ocean. MP has been detected in snow before using different methodologies. The first study on snow by Bergmann et al. (2019) showed the presence of plastic polymers in snow from the high Arctic and central Europe using FTIR. The presence of MPs in snow from the Swiss Alps used mass spectrometry for MP detection (Materić et al., 2020). Based on the limited number of studies available and the lack of a harmonized sampling- and MP determination protocol, snow as wet deposition acting as a vector for MP transport is still a relatively unexplored area of research.

In this thesis, we developed a method using acknowledged snow sampling techniques and the lipophilic staining chemical NR to identify and quantify microplastics. The method was tested by trials with NR on a range of plastic polymers and exclusion of organic material (3.6), followed by optimizing all sample handling steps from sampling in the field (3.1), storage (3.3), sample treatment for MP enrichment (3.7, 3.8) and MP determination (3.6, 3.10). Also, we developed a strict QA/QC protocol to ensure the minimization of contamination risk (3.2, 3.9).

The method was thereafter used to compare the occurrence of MPs in low-Arctic snow collected in rural and urban locations. We sampled 10 locations consisting of three subsamples per site, from which five aliquots were taken. With the optimized method, we could process one location per day (15 aliquots from subsamples, five aliquots from the field blank, and one aliquot from lab blank). The developed particle counting method can analyze ~50 filters per hour. The strict QA and QC regime that we developed reduced the contamination risk by particles during the complete sample handling process to a mean of 46 particles 100 ml<sup>-1</sup> from field samples and 21 particles 100 ml<sup>-1</sup> from the laboratory process. Resulting in a fieldblank of 184 particles 100 ml<sup>-1</sup>.

## 5.1 Method adaptation

### 5.1.1 Internal suitability of NR staining

The successful staining of known plastic polymer types by NR proved its efficacy to stain plastic particles at concentrations of  $10 \text{ mg L}^{-1}$ . Rubber from car tires did not react with NR. Rubber from car tires are in a major source of MPs to the environment (Kole et al., 2017), and therefore represents a drawback on the use of NR to stain environmental samples. Another drawback is that NR also stains cellulose that could potentially be present in the snow that is close to vegetation. To exclude some possible naturally occurring substances, grass, leaves, and bark were stained with NR, but they did not cause any fluorescence. There are possibilities to remove organic material from a sample with acid digestion (Claessens et al., 2013), alkaline digestion (Dehaut et al., 2016), or enzymatic degradation (Löder et al., 2017). As we did not expect NR to stain the organic material that was potentially present in the snow sampled, we did not treat our samples. Additionally, sample treatment has the possibility to damage plastic polymers. Ryan et al. (2019) found that acid digestion was not suitable for isolation of MPs, alkaline digestion was more suited, however there were still uncertainties associated with its use. Enzymatic digestion is more appropriate and would be our recommendation if treatment of samples were to be done. It is time consuming and more expensive, but the safest approach to not damage MP during an MP isolation step (Löder et al., 2017; Ryan et al., 2019).

The goal of the sampling approach was to acquire enough samples for analysis. The number of sites sampled for the study was 10. Two additional locations (not included in the study) were used to develop and refine the NR staining and test different aliquot volumes. An aliquot volume of 100 ml was decided upon, and five aliquots per subsample filtered to account for high intra-subsample variation. The filtration was a standard filtration method with glass equipment, glass fiber filters, and a vacuum pump. An automated counting method was developed with the use of a JavaScript macro in ImageJ, that allowed for fast and reliable counting of images. QA and QC were implemented by reducing the amount of plastic on equipment used in the field sampling and laboratory process and by taking blank samples at every step of the process to gain information about the contamination in sampling and sample handling.

### **5.1.2 Determination of the MP count**

The MDL calculated from the field blank samples was 184 particles 100 ml<sup>-1</sup>. In order to maximize our confidence in the automated count of MP, the threshold of the particle count was set to 100 (out of 255) light intensity, effectively removing all pixels that are dark from the particle count. As background noise still could present as an issue, only MP that consisted of three or more pixels were counted. The three pixels do not need to be connected in a straight line to be counted, meaning that the lowest diameter measured was two pixels. Although the protocol does not allow the identification of size classes below 22 µm, it remains a good tool to identify differences in MP concentrations above that limit. Counting visually introduces human bias to the count. Comparing the manual count to the automatic count, it was apparent that ImageJ consistently counted lower numbers (Figure 17). The significantly lower count was because ImageJ had strict counting criteria, while the human eye cannot differentiate as accurately. The counting and recording of sizes with ImageJ provided consistent results, making them comparable. The thresholds set in ImageJ were strict; this ensured that the ImageJ count was a conservative number. As the threshold applied was the same for all samples, the counted numbers were comparable between the sites. Lenz et al. (2015) also found a discrepancy between the manual and automatic count, however more related to if a particles are plastic polymers or not. In our study background noise could be counted as MPs and the threshold distinguishes between particles and background noise.

### **5.1.3 Comparability with other MP detection methods**

The staining of plastic particles with NR has been used successfully in several studies (Erni-Cassola et al., 2017; Maes et al., 2017; Shim et al., 2016). The repeated use of NR in studies on microplastic confirms its suitability. However, some flaws with inadvertent staining of particles that are not plastic have been uncovered. NR staining of microplastic particles has been validated for environmental media by two studies. Maes et al. (2017) validated the use of NR to stain plastic, by both demonstrating that NR did not stain other matter present in their samples and by validating their results with FTIR spectroscopy. Erni-Cassola et al. (2017) validated the identification of MPs with Raman spectroscopy. Both studies concluded that the NR staining of MPs is a quick and effective method to identify and count MP particles in environmental media but cautioned about possible false positives. Maes et al. (2017) uncovered that NR potentially could be used to differentiate between polymers but limited to polarity differences in plastic polymers.

## 5.2 Application of the method for the determination of MPs in snow

After subtracting the MDL, 95.4% of the aliquots were above the limit of detection. After correcting the number of MP particles for snow density, the numbers of MPs ranged from 0 to 1802 particles L<sup>-1</sup> of snow. The standard deviations for both the urban and rural locations were higher than 50% of the number of particles observed. The largest MP particle recorded was from an urban station and measured 7983 µm, while the smallest particles recorded were at the lowest resolution of the method, i.e. 22 µm.

### 5.2.1 Amount of microplastics in rural and urban areas

In this study, we found a significantly higher number of MP particles in the snow of urban areas compared to rural areas. We found a mean of 681±375 particles L<sup>-1</sup> in urban samples and a mean of 439±286 particles L<sup>-1</sup> in rural samples. The standard deviation was higher in rural samples (375) than in urban samples (286) (Figure 13). The proportion of the standard deviation compared to the mean number of MPs was lower in the urban sites (55%) than in rural sites (65%). The high difference between subsamples within locations show that microplastic particles in snow has a heterogenic distribution. With a heterogenic distribution it is important to make sure the sample volume is sufficient enough to compensate for the MP distribution within snow. Also, the high standard deviation observed in this study highlights the importance of having a sufficient number of subsamples at all sampling locations. These results suggest that both the urban and rural areas are strongly influenced by local pollution. Although the rural sites had fewer local pollution sites close by (~40km to Tromsø city), the lower number of MPs in the rural site suggests that they can have traveled with atmospheric transport. As none of the rural sampling sites were further than 40 km away from the city, it cannot yet be classified as LRT. Indeed, evidence of LRT of MPs requires snow samples from remote sites like in the high Arctic or sampling a gradient away from a source site until stable background levels can be reached.

Our findings are similar to a study performed in Paris, France, where suburban areas showed a significantly smaller amount of MP particles in the rain and dry deposition compared to dense urban areas (Dris et al., 2016). Dris et al. (2016) found that in the urban areas there was an average atmospheric fallout of 110 ± 96 particles/m<sup>2</sup>/day, while in the suburban areas it was 53 ± 38 particles/m<sup>2</sup>/day. The authors suggested that there was a more substantial amount of



local pollution in the urban areas, causing a higher concentration of plastic particles in atmospheric fallout (Dris et al., 2016).

Bergmann et al., (2019) recorded MP concentrations comparing high arctic locations to locations in central Europe and reported a significantly higher number of particles for central Europe. Their findings are presented in particles per liter of melted snow while ours are presented in particles per liter of snow. For ease of comparison, we recalculated our numbers presented in this section to particles per liter of meltwater. The number of particles Bergmann et al. (2019) found in the Arctic ranged from 0 to  $14.4 \times 10^3$  particles  $L^{-1}$ . In central Europe, the number ranged from  $0.19 \times 10^3$  to  $154 \times 10^3$  particles  $L^{-1}$ . We found on average of  $2.27 \pm 0.14 \times 10^3$  particles  $L^{-1}$  in the urban locations and  $1.24 \pm 0.15 \times 10^3$  particles  $L^{-1}$  in the rural locations. The number of particles reported is difficult to compare, as the FTIR spectroscopy used in Bergmann et al. (2019) had a higher resolution and could detect MPs down to 11  $\mu m$  while our smallest MP size detected was 22  $\mu m$ .

Nevertheless, our results are within the same order of magnitude as Bergmann's results, confirming the applicability of our method. This is to be expected, as our locations are neither in the high Arctic nor in central Europe. Our urban samples are most likely more influenced by local pollution than those of Bergmann et al. (2019), and they do not span over such a large geographical area. The number of data points in our study is, however, increasing the confidence in our findings. The number of datapoints accounts for the variation between subsamples and the variation between aliquots. The rigorous QA and QC have proved to be vitally necessary as the contamination during every sample handling step can have a large impact (Figure 15).

In general, snow density varies depending on several environmental conditions like wind, temperature, and exposure to the sun. This most likely affects the concentrations of particles found in the snow. For this reason, we highly recommend that snow density is measured as a supporting variable and that the number of particles is corrected for this parameter.

Comparing the number of particles per liter of snow instead of per liter of meltwater accounts for the varying snow densities recorded between locations. We also stress the importance of having a sufficient number of subsamples to account for the heterogenic distribution of MP in snow.

### **5.2.2 Size classes of MP particles in urban and rural stations**

The MPs found in the urban locations had a significantly larger mean size than those found in the rural locations. We predicted that the average size of MPs in rural locations would be smaller. Although the difference in size was statistically significant, the difference was only 3.07  $\mu\text{m}$ , which is not enough to fully support our assumption. Also, the smallest size class represented the highest proportion in the rural areas (Figure 14), potentially responsible for the observed difference in average size between areas, and caused by the higher potential of smaller, lighter particles to travel farther by air than larger particles. For most other size classes, urban areas exhibited the highest proportion. While Bergmann et al. (2019) did record the sizes of MP particles, they did not compare the MP sizes between central Europe and the Arctic. Bergmann et al. (2019) found MP particles ranging from 11 to 465  $\mu\text{m}$  in length, and fibers ranging from 65-14,314  $\mu\text{m}$  in length. Their proportion of MP lengths followed a similar power-law distribution as we found. Whether MPs found in the Arctic are significantly smaller than in central Europe remains to be documented. Nevertheless, we expect MP particles found in remote areas to be smaller and lighter than those found in more densely populated areas.

### **5.3 Study conclusion**

The main aim of the thesis was to establish a protocol for MPs in snow samples that is inexpensive, robust, and easy to use. The study comparing the urban and rural locations in Troms county was carried out in addition to prove the applicability and the ease of the method. The results of our study are conservative and most likely not fully representative of the real MP concentration in snow. However, they give an essential indication of the range in particle numbers and sizes to expect. Experience gained during the trial was used to refine the protocol. The protocol provides a method that can be used with commonly available equipment, both for sampling and laboratory procedures. As the snow samples can be stored in a cold room ( $-5^{\circ}\text{C}$ ), it is also possible to preserve samples over time. The most important aspects are related to QA and QC, the use of a clean-room/ -chamber is not strictly necessary, and if not available, the contamination must be estimated rigorously by having many blank samples.

## **5.4 Perspective for future research and practice**

To gain a holistic understanding of the potential LRT of MPs, the harmonization of methods in MP research is essential. In this thesis, we developed a protocol that can be used anywhere if standard laboratory equipment is available, without the need for expensive analytical equipment and requiring specialized staff to operate. Making raw data of particle counting available is also of importance as to compare studies and make inferences, notably as the resolutions increase and sizes reported become smaller. If LRT of MPs is to be investigated, a large-scale sampling effort must be performed, including several cities and remote areas, while taking meteorological conditions into account. Fresh snow sampling would also be of interest as it would create a more accurate picture of MPs present in the atmosphere at a given time.

## 6 Conclusion

The method developed proved to work efficiently, as it was not arduous to apply for neither the snow sampling nor the laboratory procedure. It should be considered as a tool in MP research. The lack of specialized equipment makes the method available for use in the most basic of research environments. The resolution of the method can be improved notably by increasing either camera resolution or magnification. With the use of an electronically controlled moving stage on the stereomicroscope, filters can be photographed in the same manner. This would allow the increase of magnification, and we could theoretically measure MPs down to 3  $\mu\text{m}$ .

Even though the data from this study are not enough to support the theory of atmospheric LRT of MPs, we could identify differences between urban and rural locations. This is revealing that local pollution impacts the number of MPs in snow. The presence of MPs in rural locations can be indicative of atmospheric transport. However, we still assume a substantial part of the MPs to come from local terrestrial pollution.

## References

- Andrady, A. L. (2011). Microplastics in the marine environment. *Marine Pollution Bulletin*, 62(8), 1596–1605. <https://doi.org/10.1016/j.marpolbul.2011.05.030>
- Barboza, L. G. A., Dick Vethaak, A., Lavorante, B. R. B. O., Lundebye, A.-K., & Guilhermino, L. (2018). Marine microplastic debris: An emerging issue for food security, food safety and human health. *Marine Pollution Bulletin*, 133, 336–348. <https://doi.org/10.1016/j.marpolbul.2018.05.047>
- Bergmann, M., Mützel, S., Primpke, S., Tekman, M. B., Trachsel, J., & Gerdts, G. (2019). White and wonderful? Microplastics prevail in snow from the Alps to the Arctic. *Science Advances*, 5(8), eaax1157. <https://doi.org/10.1126/sciadv.aax1157>
- Boucher, J., & Friot, D. (2017). Primary microplastics in the oceans: A global evaluation of sources. In *Primary microplastics in the oceans: A global evaluation of sources*. IUCN International Union for Conservation of Nature. <https://doi.org/10.2305/IUCN.CH.2017.01.en>
- Browse, J., Carslaw, K. S., Arnold, S. R., Pringle, K., & Boucher, O. (2012). The scavenging processes controlling the seasonal cycle in Arctic sulphate and black carbon aerosol. *Atmospheric Chemistry and Physics*, 12(15), 6775–6798. <https://doi.org/10.5194/acp-12-6775-2012>
- Claessens, M., Van Cauwenberghe, L., Vandegehuchte, M. B., & Janssen, C. R. (2013). New techniques for the detection of microplastics in sediments and field collected organisms. *Marine Pollution Bulletin*, 70(1–2), 227–233. <https://doi.org/10.1016/j.marpolbul.2013.03.009>
- Cózar, A., Martí, E., Duarte, C. M., García-de-Lomas, J., van Sebille, E., Ballatore, T. J., Eguíluz, V. M., González-Gordillo, J. I., Pedrotti, M. L., Echevarría, F., Troublè, R., & Irigoien, X. (2017). The Arctic Ocean as a dead end for floating plastics in the North Atlantic branch of the Thermohaline Circulation. *Science Advances*, 3(4), e1600582. <https://doi.org/10.1126/sciadv.1600582>
- Dehaut, A., Cassone, A.-L., Frère, L., Hermabessiere, L., Himber, C., Rinnert, E., Rivière, G., Lambert, C., Soudant, P., Huvet, A., Duflos, G., & Paul-Pont, I. (2016). Microplastics in seafood: Benchmark protocol for their extraction and characterization. *Environmental Pollution*, 215, 223–233. <https://doi.org/10.1016/j.envpol.2016.05.018>
- Dris, R., Gasperi, J., Saad, M., Mirande, C., & Tassin, B. (2016). Synthetic fibers in atmospheric fallout: A source of microplastics in the environment? *Marine Pollution Bulletin*, 104(1–2), 290–293. <https://doi.org/10.1016/j.marpolbul.2016.01.006>
- Eriksen, M., Maximenko, N., Thiel, M., Cummins, A., Lattin, G., Wilson, S., Hafner, J., Zellers, A., & Rifman, S. (2013). Plastic pollution in the South Pacific subtropical gyre. *Marine Pollution Bulletin*, 68(1–2), 71–76. <https://doi.org/10.1016/j.marpolbul.2012.12.021>
- Erni-Cassola, G., Gibson, M. I., Thompson, R. C., & Christie-Oleza, J. A. (2017). Lost, but Found with Nile Red: A Novel Method for Detecting and Quantifying Small Microplastics (1 mm to 20 µm) in Environmental Samples. *Environmental Science & Technology*, 51(23), 13641–13648. <https://doi.org/10.1021/acs.est.7b04512>
- Eunomia. (2016). *Eunomia (2016) Plastics in the Marine Environment* (Issue June). [www.eunomia.co.uk](http://www.eunomia.co.uk)

- Fierz, C., Armstrong, R., Durand, Y., & Etchevers, P. (2009). *The International Classification for Seasonal Snow on the Ground: Vol. IHP-VII Te*.  
<https://unesdoc.unesco.org/ark:/48223/pf0000186462>
- Gallet, J. C., Bjorkman, M. P., Larose, C., Luks, B., Martma, T., & Zdanowicz, C. (2018). *Protocols and recommendations for the measurement of snow physical properties, and sampling of snow for black carbon, water isotopes, major ions and microorganisms*.  
<http://hdl.handle.net/11250/2486183>
- Geyer, R., Jambeck, J. R., & Law, K. L. (2017). Production, use, and fate of all plastics ever made. *Science Advances*, 3(7), e1700782. <https://doi.org/10.1126/sciadv.1700782>
- Hall, N. M., Berry, K. L. E., Rintoul, L., & Hoogenboom, M. O. (2015). Microplastic ingestion by scleractinian corals. *Marine Biology*, 162(3), 725–732.  
<https://doi.org/10.1007/s00227-015-2619-7>
- Hepsø, M. O., Salaberria, I., Schmid, R., & Booth, A. M. (2018). Experimental weathering of microplastics under simulated environmental conditions. In *Master Thesis*. The Norwegian University of Science and Technology.
- Kanhai, L. D. K., Gardfeldt, K., Krumpfen, T., Thompson, R. C., & O'Connor, I. (2020). Microplastics in sea ice and seawater beneath ice floes from the Arctic Ocean. *Scientific Reports*, 10(1), 5004. <https://doi.org/10.1038/s41598-020-61948-6>
- Keller, A. S., Jimenez-Martinez, J., & Mitrano, D. M. (2020). Transport of Nano- and Microplastic through Unsaturated Porous Media from Sewage Sludge Application. *Environmental Science & Technology*, 54(2), 911–920.  
<https://doi.org/10.1021/acs.est.9b06483>
- Kole, P. J., Löhr, A. J., Van Belleghem, F., & Ragas, A. (2017). Wear and Tear of Tyres: A Stealthy Source of Microplastics in the Environment. *International Journal of Environmental Research and Public Health*, 14(10), 1265.  
<https://doi.org/10.3390/ijerph14101265>
- Lenz, R., Enders, K., Stedmon, C. A., Mackenzie, D. M. A., & Nielsen, T. G. (2015). A critical assessment of visual identification of marine microplastic using Raman spectroscopy for analysis improvement. *Marine Pollution Bulletin*, 100(1), 82–91.  
<https://doi.org/10.1016/j.marpolbul.2015.09.026>
- Löder, M. G. J., Imhof, H. K., Ladehoff, M., Löschel, L. A., Lorenz, C., Mintenig, S., Piehl, S., Primpke, S., Schrank, I., Laforsch, C., & Gerdts, G. (2017). Enzymatic Purification of Microplastics in Environmental Samples. *Environmental Science & Technology*, 51(24), 14283–14292. <https://doi.org/10.1021/acs.est.7b03055>
- Maes, T., Jessop, R., Wellner, N., Haupt, K., & Mayes, A. G. (2017). A rapid-screening approach to detect and quantify microplastics based on fluorescent tagging with Nile Red. *Scientific Reports*, 7(1), 44501. <https://doi.org/10.1038/srep44501>
- Materić, D., Kasper-Giebl, A., Kau, D., Anten, M., Greilinger, M., Ludewig, E., van Sebille, E., Röckmann, T., & Holzinger, R. (2020). Micro- and Nanoplastics in Alpine Snow: A New Method for Chemical Identification and (Semi)Quantification in the Nanogram Range. *Environmental Science & Technology*, 54(4), 2353–2359.  
<https://doi.org/10.1021/acs.est.9b07540>
- Maximenko, N., Hafner, J., & Niiler, P. (2012). Pathways of marine debris derived from trajectories of Lagrangian drifters. *Marine Pollution Bulletin*, 65(1–3), 51–62.  
<https://doi.org/10.1016/j.marpolbul.2011.04.016>
- Neves, D., Sobral, P., Ferreira, J. L., & Pereira, T. (2015). Ingestion of microplastics by commercial fish off the Portuguese coast. *Marine Pollution Bulletin*, 101(1), 119–126.  
<https://doi.org/10.1016/j.marpolbul.2015.11.008>

- Obbard, R. W., Sadri, S., Wong, Y. Q., Khitun, A. A., Baker, I., & Thompson, R. C. (2014). Global warming releases microplastic legacy frozen in Arctic Sea ice. *Earth's Future*, 2(6), 315–320. <https://doi.org/10.1002/2014EF000240>
- Rillig, M. C. (2012). Microplastic in Terrestrial Ecosystems and the Soil? *Environmental Science & Technology*, 46(12), 6453–6454. <https://doi.org/10.1021/es302011r>
- Ryan, P., Shim, W., Zhang, W., Mason, S., Galgani, F., Turra, A., Kershaw, P., Hong, S., Hassellöv, M., Lusher, A., Thiel, M., Eriksen, M., Takada, H., Tahir, A., Wilcox, C., Hardesty, B., & Uhrin, A. (2019). *GESAMP 2019 Guidelines for the monitoring & assessment of plastic litter in the ocean Reports & Studies 99* (editors Kershaw, P.J., Turra, A. and Galgani, F.).
- Shim, W. J., Song, Y. K., Hong, S. H., & Jang, M. (2016). Identification and quantification of microplastics using Nile Red staining. *Marine Pollution Bulletin*, 113(1–2), 469–476. <https://doi.org/10.1016/j.marpolbul.2016.10.049>
- Sommer, F., Dietze, V., Baum, A., Sauer, J., Gilge, S., Maschowski, C., & Gieré, R. (2018). Tire Abrasion as a Major Source of Microplastics in the Environment. *Aerosol and Air Quality Research*, 18(8), 2014–2028. <https://doi.org/10.4209/aaqr.2018.03.0099>
- Sundt, P., Schulze, P.-E., & Syversen, F. (2014). *Sources of microplastic-pollution to the marine environment m321*. 86. <https://www.miljodirektoratet.no/globalassets/publikasjoner/M321/M321.pdf>
- Thomas, J. L., Polashenski, C. M., Soja, A. J., Marelle, L., Casey, K. A., Choi, H. D., Raut, J.-C., Wiedinmyer, C., Emmons, L. K., Fast, J. D., Pelon, J., Law, K. S., Flanner, M. G., & Dibb, J. E. (2017). Quantifying black carbon deposition over the Greenland ice sheet from forest fires in Canada. *Geophysical Research Letters*, 44(15), 7965–7974. <https://doi.org/10.1002/2017GL073701>
- Trevail, A. M., Gabrielsen, G. W., Kühn, S., & Van Franeker, J. A. (2015). Elevated levels of ingested plastic in a high Arctic seabird, the northern fulmar (*Fulmarus glacialis*). *Polar Biology*, 38(7), 975–981. <https://doi.org/10.1007/s00300-015-1657-4>
- Yonkos, L. T., Friedel, E. A., Perez-Reyes, A. C., Ghosal, S., & Arthur, C. D. (2014). Microplastics in Four Estuarine Rivers in the Chesapeake Bay, U.S.A. *Environmental Science & Technology*, 48(24), 14195–14202. <https://doi.org/10.1021/es5036317>





# Appendix A

## A1 Raw data

Table A 1: Table containing the raw number of particles per liter of snow. Aliquots A1-A5 are from subsample A, Aliquots B1-B5 are from subsample B and Aliquots C1-C5 are from subsample C. U1-U5 are samples from urban locations, R1-R4 are samples from rural locations. C is the control sample.

ALIQUOT	U1	U2	U3	U4	U5	R1	R2	R3	R4	C
A1	464	251	3	NA	1393	1802	634	688	438	NA
A2	382	136	351	NA	1456	327	643	507	107	NA
A3	342	698	657	NA	1053	606	398	549	0	NA
A4	385	506	360	NA	1304	393	197	227	0	NA
A5	455	597	1033	NA	1047	916	376	87	539	NA
B1	0	245	1030	518	726	NA	NA	48	273	176
B2	42	591	976	1430	307	NA	NA	59	784	294
B3	562	1247	1048	159	225	NA	NA	129	258	501
B4	834	974	1096	355	552	NA	NA	0	564	357
B5	571	537	1196	648	565	NA	NA	318	453	261
C1	690	494	865	639	1285	519	404	NA	402	339
C2	837	1080	594	408	1104	683	242	NA	248	337
C3	1207	925	591	411	1066	798	149	NA	312	382
C4	1350	837	678	322	634	1007	0	NA	471	193
C5	956	1223	801	0	285	1091	0	NA	798	156

## A2 Raw data of field blanks

Table 4: From each location 5 aliquots were taken from the fieldblank. U1-U5 are samples from urban locations, R1-R4 represent samples from rural locations.

<b>ALIQUOT</b>	<b>U1</b>	<b>U2</b>	<b>U3</b>	<b>U4</b>	<b>U5</b>	<b>R1</b>	<b>R2</b>	<b>R3</b>	<b>R4</b>
<b>1</b>	60	180	56	77	75	53	176	101	44
<b>2</b>	54	94	51	28	66	51	83	128	47
<b>3</b>	49	92	36	26	22	27	112	120	33
<b>4</b>	63	67	47	175	40	37	43	55	32
<b>5</b>	86	77	61	65	5	85	59	35	56

## Appendix B

# Protocol for detection of microplastics in snow

---

## Introduction

Microplastics in the snow is a new field in plastics research; this protocol is, therefore, a contribution to standardizing methods. Contamination in plastics research is a widespread issue, and the protocol will include blank samples at all stages of the sampling and analyzation process.

Microplastic present in snow can have several origins, where local contamination and atmospheric transport are suspected to be the main sources. Local contamination would contribute to larger microplastics and macro plastics. Snow acts as a scavenger of particles suspended in the air. If the wind transports microplastics, they should be found in the snow, and these will probably range from small size microplastics to nano plastics.

The method of sampling is based on (Gallet et al., 2018), with some adaptations made to account for the plastic contamination of the samples and explaining the process for determining if there are microplastics in the sample.

## QA and QC for field sampling

### Avoiding and testing contamination

During the sampling procedure, there is a high chance of self-contamination. Most of the tools used should not be made out of any plastic components. The problem is the container used for the snow, whirl-pak 550 consisting of **low-density polyethylene** (LDPE), which possibly will contaminate the sample. Excavate the snow pits using a shovel made of steel or a metal alloy to avoid plastic contamination from the shovel. Clothes worn during the sampling could also lead to possible contamination. Contamination by clothes will mostly be microfibers. Avoid plastic contamination by wearing natural fibers (wool, cotton, etc.) to reduce the direct contamination of the sample. Since plastic makes up almost all products we associate with daily, there are many possible sources for contamination which makes investigation of microplastics difficult.

To see if there is any contamination during sampling or laboratory processing, there will have to be several blank samples. When taking snow samples, an open bag will be placed on the side of the excavation to catch any contamination when taking the snow samples.

## Preparation for snow sampling

### Metadata

1. Note GPS coordinates with the geoid reference system (ex. WGS84, NAD84).
2. Take photos of sampling sites and notation of possible local contaminants and distance to them, most important roads, buildings, and other obstructions.
3. Take a photo of clothes worn during sampling or a notation of what material they consisted of.
4. Estimate and note down the distance to local variations such as open ground, open water, anything that could impact snowpack conditions.
5. Record meteorological conditions such as time since last snowfall, wind direction, cloud cover, or direct sunlight.

### Sampling equipment

Snow sampling does not require a large amount of specialized equipment. Dealing with microplastic sampling does require a particular emphasis on limiting contamination. The equipment has to be as plastic-free as possible to decrease contamination.

**Shovels** made of mainly aluminum or steel, and they need to be sturdy as this is one of the tools that is most likely to break; bringing several will decrease the risk of sampling failure.

**Snow saws** can be useful to create clean edges and break harder layers.

**Foldable ruler or avalanche probe** with measurements to measure snow depth. Avalanche probes are more useful than foldable rulers as they tend to break in cold and wet conditions. If Avalanche probes are not available, bring several foldable rulers.

**Thermometer** with wit external probe to measure temperature within the snow layers.

**Snow density tool** can be acquired from snowmetrics (rip cutter) or a metal tube with known weight and volume.

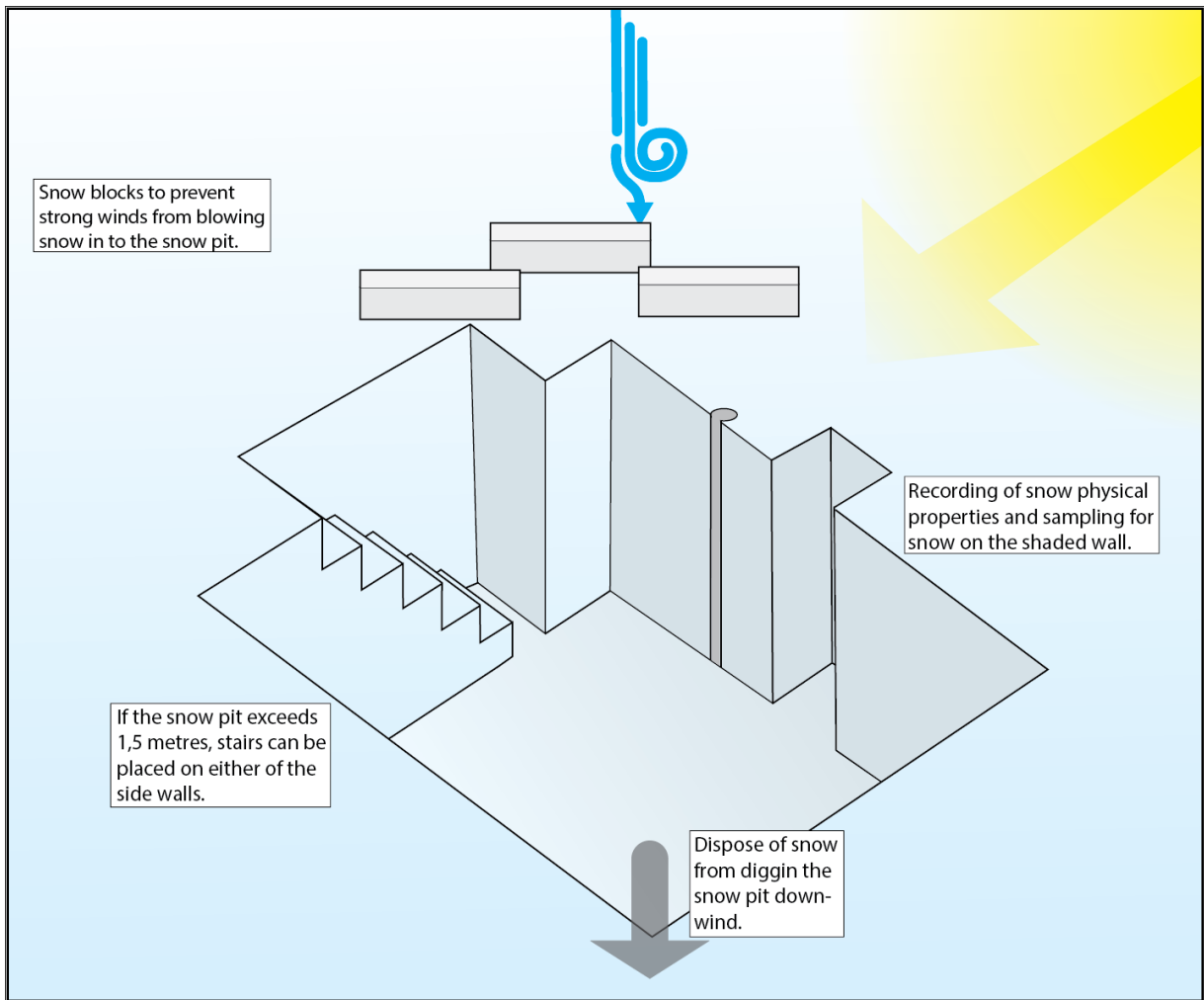
**Weight scale** to weigh snow in the snow density tool. The resolution of the scale varies depending on the volume of the snow density tool. For 0.5 L of snow, a resolution of 1 gram is enough.

**Sampling containers** for snow. Such as the whirl pak 550. Metal or glass containers are more advantageous, but they are unpractical. Use an appropriate container to get an adequate amount of snow and fits the practicalities of fieldwork.

## **Recommendations on digging snow pits**

For high-quality samples, snow pits must be excavated with care following certain precautions to limit contamination and correctly measure snow physical properties.

1. The orientation of the snowpit should be towards the sun, with the wall on which sampling will take place being in the shade.
2. Snow extracted by creating the snow pits has to be disposed of downwind as far away as possible to avoid snow drifting back into the pit.
3. Snow pits have to be large enough, so movement is not restricted, and there is space to complete sampling without touching the walls.
4. On days with strong winds, it might be useful to create walls upwind of the snow pit to shelter sampling from the wind. It is essential to not trample the area above the wall where sampling is going to take place.
5. On glaciers and areas where the snow is older than one year, it is important to dig down to the snow-firn-ice transition, if the pit is deeper than one metre, stairs or a ladder might be of use.



### Sampling for snow

	Temperature	Snow hardness	Snow density	Snow sample
10 cm				
20 cm				
30 cm				
40 cm				
ice/ground				

whirlpak

## Temperature

Measure the **temperature** at **first** because the walls quickly increase or decrease in temperature when exposed to the surrounding environment (Gallet et al., 2018).

Take temperature measurements every 5 centimeters at the top 20 centimeters, and then one measurement for each discrete layer with at least one measurement for every 10 centimeters.

## Snow stratigraphy

Use a ruler to record the depth of each measurement and stratigraphy, 0 cm is always on the top of the snowpit (**0cm = surface of the snowpit**). Snow hardness is the simplest of the snow stratigraphic parameters to record, and it does not require any specialized equipment, only a pen, and a knife. Insert objects from largest to smallest into the snow following table 1. Record which objects successfully entered to estimate snow hardness throughout the column.

Term	Hand hardness test			Ram <sup>2</sup> test (N)		Symbol
	Index	Object	Code	Range	Mean	
Very soft	1	Fist	F	0-50	20	/
Soft	2	4 fingers	4F	50-175	100	X
Medium	3	1 finger	1F	175-390	250	//
Hard	4	Pencil <sup>1</sup>	P	390-715	500	☒
Very Hard	5	Knife blade	K	715-1200	1000	■
Ice	6	Ice	I	>1200	>1200	○

**Table 1.** Recommended hardness scale from (Fierz et al., 2009)

## **Snow density**

Measure snow density for the whole snow column. The simplest way is to use a steel tube with a known length and radius to calculate the volume. The larger the amount, the less the margin of error, use a high-resolution scale if snow density tool is low volume.

The first step is to weigh the empty tube on the scale and noting down its weight that will be subtracted later. Then insert the tube into the snow and block the lower end and weigh the tube with the snow inside.

If there are hard or icy layers, a sturdy tube can be hammered to break through more robust layers. If this is not possible, use a snow saw to cut out a piece, measure its dimensions and weight to calculate its density.

After the weight of each layer is recorded using a simple equation for density calculation.

$$Density \left( \frac{gr}{l} \right) = \frac{snow\ mass\ (gr)}{volume\ of\ tool\ (l)}$$

Measuring snow density is an essential step as it will enable you to calculate the number of microplastics or other particles per unit of volume.

## **Sampling for plastic particles**

The suggested bag for sampling snow samples are the 5441 ml whirl-pak bags. The amount of snow to be sampled has to be relatively high to assure a higher rate of microplastics per sample as the expected levels in snow are low. The amount of meltwater from a given snow sample is dependent on the density.

To make sure that you get a sample from the whole snow column transfer small amounts each time to fill the bag up as much as possible with an even amount from each layer. At each site, take three subsamples. When doing one of the samples open up a second sampling bag that will be open during the whole procedure, this will be used as a blank sample to correct any results for self-contamination.

It is important to stress the fact that the equipment used for snow samples have to be as plastic-free as possible, and if there is any unnecessary plastic equipment nearby that this is stored a couple of meters away downwind. If the samples are analyzed for polymer type, test



the equipment so that those polymers can be taken into account as possible self-contamination.

## **QA and QC for Laboratory procedures**

### **Avoiding and testing for contamination**

Laboratory processes can contribute a substantial input of microplastic particles, potentially influencing results. There are two ways to counteract the contamination, blank samples, and working on the sample in an environment with a low amount of plastic. Do blank samples either way, and they should preferably account for all equipment used and represent the whole laboratory procedure after opening the sample containers. Processing samples in a cleanroom is advantageous if it is equipped with overpressure to keep particles out and a particle filter to filter ingoing air. The use of a laminar flow cabinet can replace a clean room as long as the flow is going out and not in.

### **Preparation of laboratory analysis filtration and staining equipment**

- Glass pipettes
- Erlenmeyer flask
- 250ml beakers
- 500ml funnel
- Clamps
- Compressor base
- 47mm GFF filters
- Metal tweezers
- Tinfoil
- Vacuum pump
- Nile red
- Ethanol
- Brown glass jars

All filters and equipment made out of glass or metal should be burned before use to rid it of any plastic residue.

### **Melting of snow**

Snow samples should be thawed at room temperature without external heat applied, to protect the sampling container and limit the number of particles coming off the bags. For samples

stored below freezing, there is a risk of snow having sharp edges that puncture the bags. To ensure that the bags do not leak during melting, pack the sample in a second bag.

## **Nile red solution**

Mix 3 mg, technical grade Nile red with 300 ml ethanol to create a 0.1 mg/ml solution. When the Nile red is diluted, filter the solution with a GFF filter to remove any plastic particles.

## **Laboratory analysis of snow samples**

### **Filtration and staining**

Decide the desired sub-sample size and retrieve it from the melted samples. Make sure that the subsample size does not contain too many particles to avoid stacking. Trial runs should be performed for new samples to decide what volume works the best.

Samples are filtered through GFF filters in the filtration setup with a compressor pump. After releasing a vacuum, use a glass pipette for bathing the filter in a layer of Nile red solution and letting it stain for 5 minutes. Turn on the compressor pump to remove any excess Nile red solution and then rinse the filter to remove any leftover color on the filter. Pack filters in aluminum foil to prevent exposure to plastic particles and light.

### **Visual analysis**

The plastic particles stained with Nile red will only light up under blue light. LEDs with a wavelength between 450 and 510 nm will excite the dye (Erni-Cassola et al., 2017). An orange filter is needed to remove out the blue light leaving only the stained particles visible.

Using a stereomicroscope or similar equipped with a camera, take pictures to cover the entire filter at desired magnification.

### **Counting stained microplastics from pictures**

To make the counting process efficient we recommend that pictures are transformed in to black and white in Adobe Lightroom. This also allows for removing parts of the picture that are not of the filter itself. This is highly recommended to exclude false positives. Counting from pictures can be to some extent be automated using ImageJ. It is important to make sure that pictures are taken with the same microscope settings for the count to be continually accurate. Depending on the light conditions the thresholds should be tested before using the

script. This can be done by applying the thresholds manually in ImageJ. Adapt the script provided to your file paths in the computer, and test it. To get output about diameter of the particles recorded a setting in ImageJ has to be enabled previous to running a script. This is found under Analyze->Set Measurements and tick the box for Ferets diameter. When this box is ticked all .CSV files exported will contain the longest diameter recorded for each microplastic particle.

## References

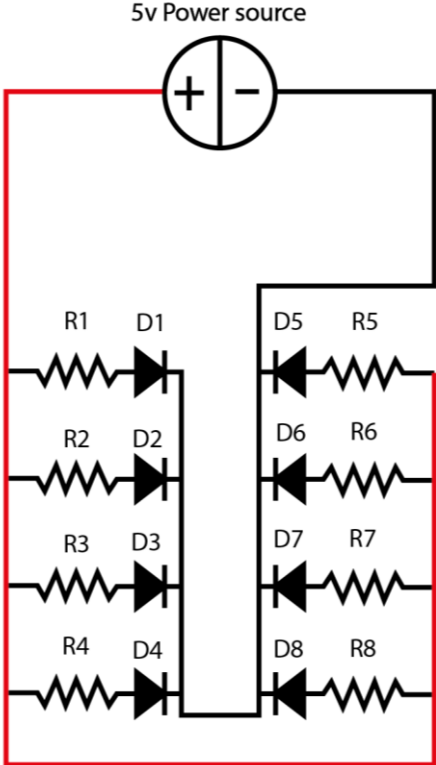
- Erni-Cassola, G., Gibson, M. I., Thompson, R. C., & Christie-Oleza, J. A. (2017). Lost, but Found with Nile Red: A Novel Method for Detecting and Quantifying Small Microplastics (1 mm to 20  $\mu\text{m}$ ) in Environmental Samples. *Environmental Science & Technology*, 51(23), 13641–13648. <https://doi.org/10.1021/acs.est.7b04512>
- Fierz, C., Armstrong, R., Durand, Y., & Etchevers, P. (2009). *The International Classification for Seasonal Snow on the Ground: Vol. IHP-VII Te*. <https://unesdoc.unesco.org/ark:/48223/pf0000186462>
- Gallet, J. C., Bjorkman, M. P., Larose, C., Luks, B., Martma, T., & Zdanowicz, C. (2018). *Protocols and recommendations for the measurement of snow physical properties, and sampling of snow for black carbon, water isotopes, major ions and microorganisms*. <http://hdl.handle.net/11250/2486183>

## Appendix C

### Macro for ImageJ

```
macro "Automated-Particle-Analysis" {
inputFolder=getDirectory("C:/"insert your picture folder path here");
outputFolder=getDirectory("C:/"insert your output folder path here");
list=getFileList(inputFolder);
setBatchMode(true);
for(i=0; i<list.length; i++) {
  path=inputFolder+list[i];
  if(endsWith(path, ".jpg")) open(path);
  showProgress(i, list.length);
  setThreshold(100, 255);
  setOption("BlackBackground", false);
  run("Convert to Mask");
  if(nImages>=1) {
    if(i==0) {
    }
    run("Analyze Particles...", "size=3-Infinity show=Nothing display exclude clear include
record add");
    selectWindow("Results");
    outputPath=outputFolder+list[i];
    //The following two lines removes the file extension
    fileExtension=lastIndexOf(outputPath, ".");
    if(fileExtension!=-1) outputPath=substring(outputPath,0,fileExtension);
    saveAs("Measurements", outputPath+".csv");
    run("Close"); //closes Results window
    close(); //closes the current image
  }
}
setBatchMode(false);
}
```

# Appendix D



Light emitting diodes (D1-D8): 4v 450nm  
Resistors (R1-R8): 33ohm resistance

Appendix Figure D1: Wiring diagram for LED used in the stereomicroscope attachment.



